[Palaeontology, Vol. 49, Part 4, 2006, pp. 695–718]

THE POSTCRANIAL SKELETON OF THE HYPOSAURINAE (DYROSAURIDAE; CROCODYLIFORMES)

by DANIELA SCHWARZ*, EBERHARD FREY† *and* THOMAS MARTIN‡

*Naturhistorisches Museum Basel, Augustinergasse 2, CH-4001 Basel, Switzerland; e-mail: Daniela.Schwarz@bs.ch
†Staatliches Museum für Naturkunde Karlsruhe, Erbprinzenstrasse 13, D-76133 Karlsruhe, Germany; e-mail: dinofrey@aol.com
‡Forschungsinstitut Senckenberg, Sektion Mammalogie, Senckenberganlage 25, D-60325 Frankfurt am Main, Germany; e-mail: tmartin@senckenberg.de

Typescript received 12 November 2004; accepted in revised form 27 May 2005

Abstract: A detailed description of the postcranial skeleton of the Hyposaurinae is presented, based on the hitherto known and new postcranial material. The postcranial skeleton of the hyposaurine Dyrosauridae differs from that of all other crocodilians by the high neural spines, which can reach up to four times the length of the vertebral body, thoracic ribs, which are five times longer than the adjacent vertebral body, dorsal osteoderms lacking an external keel, deep haemal arches, which reach up to 3·4 times the length of the vertebral body, an ilium with a prominent craniodorsal tubercle, and a scapula with an expanded and lateromedially flattened scapular wing, which makes the scapula 1·5 times as large as the coracoid. The similarity of the postcranium of *Dyrosaurus*, *Hyposaurus*, *Congosaurus* and *Rhabdognathus* allows a uniform skeletal reconstruction for the Hyposaurinae. Only fragmentary material is known from the Phosphatosaurinae. The comparative osteological description of all hyposaurine specimens known to date establishes a basis for future constructional morphological analyses and the reconstruction of their evolutionary history.

Key words: Comparative anatomy, Crocodilia, Dyrosauridae, Hyposaurinae, osteology, skeletal reconstruction.

THE Dyrosauridae are a family of fossil longirostrine crocodilians reported from late Early Cretaceous (Cenomanian; Buffetaut and Lauverjat 1978; Buffetaut *et al.* 1990) to Early Eocene (Lutetian; Buffetaut 1978*a–c*) deposits. Remains of Dyrosauridae occur in marine, brackish and fluviatile sediments of the southern Tethys margin and the coastal regions of the Southern and Central Atlantic (Buffetaut 1976, 1978*a–c*, 1980; Langston 1995; Denton *et al.* 1997; Hua 1997).

The postcranial skeleton of the Phosphatosaurinae (Buffetaut 1980) is only known from fragmentary remains, so that a confident reconstruction of their osteology is impossible on the basis of current knowledge. This is contrasted by the Hyposaurinae (Buffetaut 1980), of which during the last few years excellently preserved postcranial material has been discovered. Based on this and previously known material, a precise skeletal reconstruction for the hyposaurine genera *Dyrosaurus* Pomel, 1894, *Congosaurus* Dollo, 1914, *Hyposaurus* Owen, 1849, and *Rhabdognathus* Swinton, 1930 is possible. The only minor structural differences between the postcranial elements of those taxa allow a revision and general reconstruction of the postcranial skeleton for the Hyposaurinae.

The postcranial skeleton of the Hyposaurinae differs from that of other crocodilians, especially in neural spines that reach a height of up to four times the length of the adjacent vertebral body. This indicates fundamental differences from extant crocodilians concerning muscle arrangement, bracing system and, as a consequence, locomotory options (Salisbury 2001; Salisbury and Frey 2001).

The first reconstruction of the postcranial skeleton of a hyposaurine crocodilian was provided by Langston (1995) for cf. *Rhabdognathus* (Text-fig. 1A). In contrast to Langston's (1995) reconstruction based on incomplete material, the reconstruction presented by Hua (1997) of a generalized skeleton of a dyrosaurid postcranium appears very simplified. The same reconstruction is referred to *Dyrosaurus* in Hua and Buffetaut (1997). These two reconstructions represent, until now, the only drawings of a skeleton of a hyposaurine dyrosaur. The apparent differences between the two reconstructions (Text-fig. 1) indicate uncertainties about the heights of the neural spines along the vertebral column. Hitherto, the morphology of the dorsal osteodermal shield was not reconstructed. Langston (1995) presented a reconstruction of three segments of the thoracic part of the dorsal armour. The

incomplete knowledge of the dyrosaurid postcranium is also mirrored in phylogenetic analyses, in which postcranial characters for Dyrosauridae are mostly coded as unknown (e.g. Pol 2003).

With the recently discovered new hyposaurine skeletons a wealth of new information on their postcranial anatomy became available. Additionally, the revision of a partial skeleton of *Congosaurus bequaerti* (MRAC; Jouve and Schwarz 2004) revealed a near complete dorsal osteodermal shield that has not been described in detail before. Comparisons with modern crocodiles were made to point out the main structural and proportional differences between the Hyposaurinae and other crocodilians. Although the skeletal reconstructions were made for the purpose of a constructional morphological analysis of the axial skeleton (Schwarz 2003), they also provide a database from which to elucidate the evolutionary history of the hyposaurine dyrosaurs.

MATERIAL AND METHODS

The material examined comprises the partial skeleton of *Congosaurus bequaerti* (MRAC 1741–1743, 1745, 1796, 1797, 1802, 1803, 1806, 1809–1811, 1813–1819, 1823, 1828, 1839, 1852, 1854, 1895, 1870, 1871, 1887, 1894) and the partial skeleton of *Dyrosaurus* sp. (SMNK-PAL 3826), as well as a wealth of isolated elements of the postcranium of *Dyrosaurus* spp. (MNHN), *Hyposaurus natator* (YPM), *Hyposaurus* spp. (AMNH, BMNH, MNHN, YPM) and *Rhabdoghathus* sp. (BMNH, MNHN). The remains of cf. *Phosphatosaurus* (MNHN), cf. *Sokotosaurus* (MNHN) and of undetermined Dyrosauridae (MNHN, BMNH) were also examined, but these did not have any impact on this study owing to the incomplete nature of the material. Information on specimens that could not be examined personally (e.g. *Dyrosaurus* spp. OCP, cf. *Rhabdognathus* Langston 1995 or cf. *Hyposaurus* Storrs 1986) was taken from photographs and from the literature.

A complete skeleton of *Crocodylus porosus* (IPFUB, OS 38) was taken as a reference for the comparison with recent crocodilians. Measurements of the angles between the articular surfaces of the zygapophyses and the median plane in the axial skeleton of *Crocodylus niloticus*, *C. siamensis* and *Gavialis gangeticus* were taken from Hua (1997, 2003). Additionally, skeletal remains of *Gavialis gangeticus* (NMB 1193) and *Tomistoma schlegeli* (NMB, no collection number) were examined.

Measurements were made with a DIN norm slide gauge, tape measure and angle rule. Within a vertebra, the length of the vertebral body was used as a reference value for the comparison of proportional relations.

The osteological description was made in context with a biomechanical analysis of a bionomic construction (Salisbury 2001) and explicitly does not express a phylogenetic hypothesis. Linnean taxonomy is followed

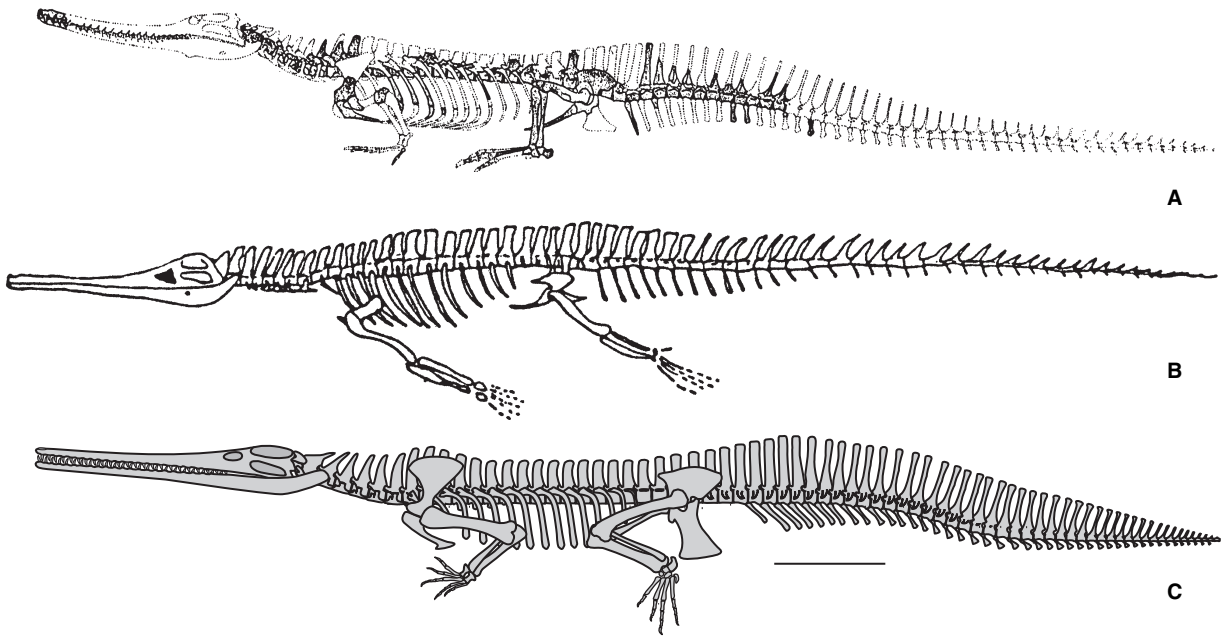

TEXT-FIG. 1. Comparison of different reconstructions of the postcranial skeleton of the Hyposaurinae. A, reconstruction of the skeleton of cf. *Rhabdognathus* after Langston (1995). B, reconstruction of a generalized dyrosaurid crocodilian after Hua (1997). C, reconstruction of *Congosaurus bequaerti* corresponding in the postcranial skeleton to a generalized hyposaurine dyrosaurid described in this paper and after Schwarz (2003). Note the differing reconstructed heights of the neural spines. Scale bar represents 0·5 m.

throughout the paper. The family Dyrosauridae was defined by Buffetaut (1976) and comprises the two subfamilies Phosphatosaurinae and Hyposaurinae (Buffetaut 1980).

Institutional abbreviations. AMNH, American Museum of Natural History, New York; BMNH/NHM, The Natural History Museum, London; IPFUB, Fachrichtung Paläontologie des Instituts für Geologische Wissenschaften der Freien Universität Berlin; MNHN, Museum National d'Histoire, Paris; MRAC, Musée Royal d'Afrique Centrale, Tervuren; NMB, Naturhistorisches Museum Basel; SMNK-PAL, Staatliches Museum für Naturkunde Karlsruhe, Paläontologische Sammlung; YPM, Yale Peabody Museum, New Haven.

Abbreviations used in the text-figures: English (Latin term) acet, acetabulum; ar lig elast, insertion scar for the ligamentum elasticum interlaminare (area ligamenti elastici); CaV, caudal vertebra (vertebra caudalis); can neu, neural canal (canalis neuralis); capm, capitulum (capitulum costae); cond lat fe/hu, lateral condyle of the distal extremity of the femur/humerus (condylus lateralis ossis femoris/ossis humeri); cond med fe/hu, medial condyle of the distal extremity of the femur/humerus (condylus medialis ossis femoris/osis humeri); c cau, caudal rib at the first to fourth caudal vertebra, separated from the vertebral body by a distinct suture (costa caudalis); CeV, cervical vertebra (vertebra cervicalis); cs 1/2, first/second sacral rib (costa sacralis 1/2); cr, crest, keel (crista); cr deltpect, deltopectoral crest (crista deltopectoralis); cr cran scap, cranial scapular crest, acromion or deltoid ridge (crista cranialis scapulae); cr supracet, supraacetabular crest (crista supraacetabularis); dep, depression (depressio); dep cau fe, caudal depression at femur (depressio caudalis ossis femoris); dep cranlat is, craniolateral depression of ischium (depressio craniolateralis ischiadicus); dep med fe, medial depression at femur (depressio medialis ossis femoris); dep prox fe, proximal depression at femur (depressio proximalis ossis femoris); dermost acc, accessory, lateral osteoderm of the dorsal osteodermal shield (dermosteum accessorium); dermost paravert, medial osteoderm of paravertebral shield (dermosteum paravertebrale); diap, diapophysis (diapophysis); DoV, dorsal vertebra (vertebra dorsalis); epc lat fe/hu, lateral epicondyle of the femur/humerus (epicondylus lateralis ossis femoris/ossis humeri); epc med fe/hu, medial epicondyle of the femur/humerus (epicondylus medialis ossis femoris/ossis humeri); f art at, articular surface for the atlas neural arch with the dens (facies articularis atlantica); f art arc haem, articular surface for the haemal arch (facies articularis arcus haemalis); f art cran, cranial articular surface at the atlas neural arch (facies articularis cranialis); f art cor, articular surface for the coracoid at the scapular head (facies articularis coracoidea); f art cs 1, articular surface for the sacral rib on the caudal surface of the vertebral body of the first praesacral vertebra (facies articularis costae sacralis 1); f art ext ost, external cranial articular surface of the osteoderm (facies articularis externa dermostei); f art int ost, internal caudal articular surface of the osteoderm (facies articularis interna dermostei); f art lat ost, lateral articular surface of the paravertebral and medial accessory osteoderms (facies articularis lateralis dermostei accessorii); f art med ost, medial articular surface of the medial and lateral accessory osteoderms (facies articularis medialis dermostei); f art fi, articular surface of tibia for fibula(facies articularis fibularis); f art hu, articular surface for the humerus at the scapula and coracoid (facies articularis humeralis); f art il, articular surface of ischium for ilium (facies articularis iliaca); f art is, articular surface of the ilium with the ischium (facies articularis ischiaca); f art pub, articular surface of ischium for pubis (facies articularis pubica); f art scap, articular surface of the coracoid head with the scapula (facies articularis scapularis); f art ti, articular surface of fibula for tibia (facies articularis tibiae); f art ul, articular surface for ulna at the radiale (facies articularis ulnae); f art v praes 1, articular surface for the first praesacral vertebra at the first sacral rib (facies articularis vertebrae praesacralis 1); f med ost, medial, bevelled face of the internal surface of the paravertebral osteoderms (facies medialis osteodermalis); f sym il, articular surface of the sacral rib with the ilium (facies symphysialis ilii); f sym s1/2, articular surface of the ilium for the first/second sacral rib (facies symphysialis costa sacralis 1/2); for cor, coracoidal foramen (foramen coracoideum); fos acet, acetabular fossa (fossa acetabularis); fos art cran, cranial articular fossa of the dens (fossa articularis cranialis); fos partroch, paratrochanterial fossa (fossa paratrochanterica); fov, fovea; fov c, costal fovea at the atlas intercentrum for the atlas cervical rib (fovea costae); hc lat/med ul, lateral/medial hemicondyle on distal extremity of the ulna (hemicondylus lateralis/medialis); hyp, hypapophysis; inc acet il/is, iliac/ischiac incision of the acetabular foramen (incisura acetabularis iliae/ischiae); inc ct, capitulotubercular incision (incisura capitulotubercularis); lin arc cranlat, prominent craniolateral crest laterally on the proximal extremity of the humerus (linea arcuata craniolateralis); lin is, curved line between craniolateral and caudolateral margin of the lateral surface of the ischium (linea arcuata ischii); ole, olecranon; parap, parapophysis; ped acet, acetabular pecuncle of the ilium (pedunculus acetabularis); postz, postzygapophysis; praez, praezygapophysis; pr, process (processus); pr c, costal process of the tail, entirely fused to the caudal vertebra (processus costalis); pr cran, cranial part of the cervical and cranial process at the cranial thoracic ribs (processus cranialis); pr glen cor, glenoid process of the coracoid (processus glenoidalis coracoidei); pr glen scap, glenoid process of the scapula (processus glenoidalis scapulae); pr spin, neural spine (processus spinosus); pr subacet is, subacetabular process of ischium (processus subacetabularis ischii); pr trans, transverse process (processus transvs.); rec postacet, caudal recess of the ilium (recessus postacetabularis); rug, rugosity (rugositas); rug cau cor, caudal rugosity of the coracoid neck (rugositas caudalis coracoidei); rug caudlat il, caudolateral rugosity at the lateral surface of the ilium (rugositas caudolateralis iliaca); rug int fe, rugosity within the intercondylar fossa of the femur (rugositas intermedia ossis femoris); rug med fe, medial rugosity of distal extremity of femur (rugositas medialis ossis femoris); rug med subacet, rugosity at the medial surface of subacetabular process of ischium (rugositas medialis subacetabularis); rug ventlat cor, prominent cranial rugosity of the ventrolateral surface of the coracoid (rugositas ventrolateralis coracoidei); sulc, groove (sulcus); sulc dist ti, distal groove on tibia (sulcus distalis tibiae); sulc dist ul, distal groove on ulna (sulcus distalis ulnae); sut nc, neurocentral suture (sutura neurocentralis); troc fe, fourth trochanter of the femur (trochanter

ossis femoris); troc fi, fibular trochanter (trochanter fibularis); tub acet, tuberosity within the acetabular fossa (tuberositas acetabularis); tub cau fe, caudal tuberosity at femur (tuberositas caudalis ossis femoris); tub caudmed cor, caudomedial tuberosity on the coracoid blade (tuberositas caudomedialis coracoidei); tub caudlat fe, caudolateral tuberosity on femur (tuberositas caudolateralis ossis femoris); tub caudlat il, caudolateral tuberosity at ilium (tuberositas caudale ilii); tub cranmed hu, craniomedial tuberosity on cranial tip of the deltopectoral crest of humerus (tuberositas craniomedialis ossis humeri); tub lat hu, lateral tuberosity of humerus (tuberositas lateralis ossis humeri); tub rec postac, tuberosity at the postacetabular recess of the ilium (tuberositas recessus postacetabularis); tub scap, lateral tuberosity between medial and mediolateral surface of the scapular head (tuberositas lateralis scapulae); tubc cau scap, ventral tuberculum at the caudal scapular margin (tuberculum caudale scapulae); tubc crandors il, craniodorsal tubercle of ilium (tuberculum craniodorsale ilii); tuber, tuber; tubm, tuberculum of rib (tuberculum costae).

COMPARATIVE OSTEOLOGY OF THE HYPOSAURINE POSTCRANIUM

Axial skeleton

Partial skeletons of *Dyrosaurus* sp. (SMNK 3826), *Congosaurus bequaerti* (Jouve and Schwarz 2004), *Hyposaurus rogersii* (Troxell 1925), cf. *Hyposaurus* (Storrs 1986) and cf. *Rhabdognathus* (Langston 1995) comprise series of cervical vertebrae, consisting of atlas, dens and axis and the third to ninth cervical vertebrae. The proatlas is only known from *Hyposaurus* (Parris 1986) and *Dyrosaurus* (S. Jouve, pers. comm. 2002). At least 16 dorsal vertebrae and two sacral vertebrae are reconstructed from the partial skeletons of *Dyrosaurus*, *Hyposaurus* (Troxell 1925; Storrs 1986) and cf. *Rhabdognathus* (Langston 1995). The first to thirty-sixth caudal vertebrae are preserved in a partial skeleton of *Congosaurus bequaerti* (MRAC). The lengths of the caudal vertebral bodies indicate a minimum number of 45 caudal vertebrae for the Hyposaurinae (see also Text-fig. 1C). The vertebral bodies of the cervical, dorsal, sacral and caudal vertebrae are weakly amphicoelous. The vertebral fossa at the cranial and caudal articular surfaces of the cervical, dorsal and caudal vertebrae bear a central, kidney-shaped fovea and is surrounded by a narrow sulcus.

Proatlas and atlas. The proatlas forms a dorsally vaulted arch. The intercentrum of the atlas of the Hyposaurinae articulates with the ventral surface of the dens and reaches one-third of the length of the axis. The intercentrum is wedge-shaped with rounded corners (Text-fig. 2A). It is dorsoventrally compressed with a height-length ratio of 1 : 2 and the sharp edge is orientated caudally. The cranial surface of the intercentrum is transversely oval and concave. In dorsal view, the intercentrum is trapezoidal, tapering from cranial to caudal for one-third of its cranial width. The lateral corners of the caudal margin are extended into a pair of blunt, caudolaterally orientated tubera that continue cranially as a pair of low cristae onto the intercentrum (Text-fig. 2A). Between these cristae, several longitudinally oval nutricious foramina are visible. Parallel to the cranial margin there is a rugosity, lateral to which longitudinally orientated striae radiate over the cranial half of the dorsal surface of the intercentrum. The foveae for the pair of atlas ribs are situated lateral to the caudal tubera and show a rugose surface.

The paired neural arch of the atlas reaches two-thirds of the height of the intercentrum of the atlas (Text-fig. 2B). The neural arch cranially articulates with the craniodorsal surface of the dens and caudally overhangs the cranial fifth of the axis neural arch. The neural arch of the atlas consists of two bilateral symmetrical arcuate elements. The cranial third of an arcuate element is massive and bears two articular facets, which are cranially and ventrally orientated, respectively (Text-fig. 2B–C). The slightly concave cranial articular surface is orientated craniomedially and shows an oval outline with the long axis orientated from ventrolaterally to dorsomedially. Lateral to the cranial articular surface there is a ventrally orientated spine, which is separated from the cranial articular surface by a narrow sulcus (Text-fig. 2C). The ventral articular surface lies caudally adjacent to the cranial articular surface and is one-tenth longer than the latter. The outline of the ventral articular surface is oval with the long axis running craniomedially to caudolaterally.

The caudal two-thirds of the arcuate element form a lamina that consists of a vertical and a horizontal part of similar size. The height of the lamina decreases by 50 per cent cranioventrally to caudodorsally. The medial surface of the lamina is deeply concave in longitudinal direction. The lateral surface of the lamina bears a triangular depression covering almost the entire surface (Text-fig. 2C). This depression is four times as large as the rounded depression in the cranial quarter of the horizontal part.

Dens and axis. The dens of the Hyposaurinae is wedge-shaped with the narrow end facing ventrally (Text-fig. 2D). Its caudal surface is strongly rugose (Text-fig. 2G; Troxell 1925; Langston 1995) in all Hyposaurinae. The morphology of its cranial surface, however, differs between the genera. In *Dyrosaurus* (SMNK-PAL 3826 (31/94)) it deepens dorsoventrally and bears a central fovea in its dorsal half (Text-fig. 2F). The cranial surface of the dens of *Congosaurus* (Text-fig. 2E; Jouve and Schwarz 2004) and *Hyposaurus* (Troxell 1925) is concave, but otherwise shows no sculpturing. In cf. *Rhabdognathus*, the cranial surface of the dens is characterised by a transversely oval depression (Langston 1995).

The axis is hour-glass-shaped in ventral view. Its width at the constriction is half its width at the caudal margin. The ventral surface of the axial body bears several longitudinally orientated crests that vary intergenerically (Langston 1995; Jouve and Schwarz 2004). A hatchet-shaped hypapophysis with rugose lateral surfaces arises from the caudal third of the ventral surface of the axis (Text-fig. 2D, H). The parapophysis of the axis contributes with its cranial half to the dens and with its caudal half to the axial body (Text-fig. 2D). The diapophysis is a prominent tuber in the dorsal half of the lateral surface of the dens (Text-fig. 2D, G).

The axial neural arch cranially overlaps the caudal fourth of the dens (Text-fig. 2D). The peduncle of the neural arch of the axis is two-fifths higher than the axial body is long. The area for

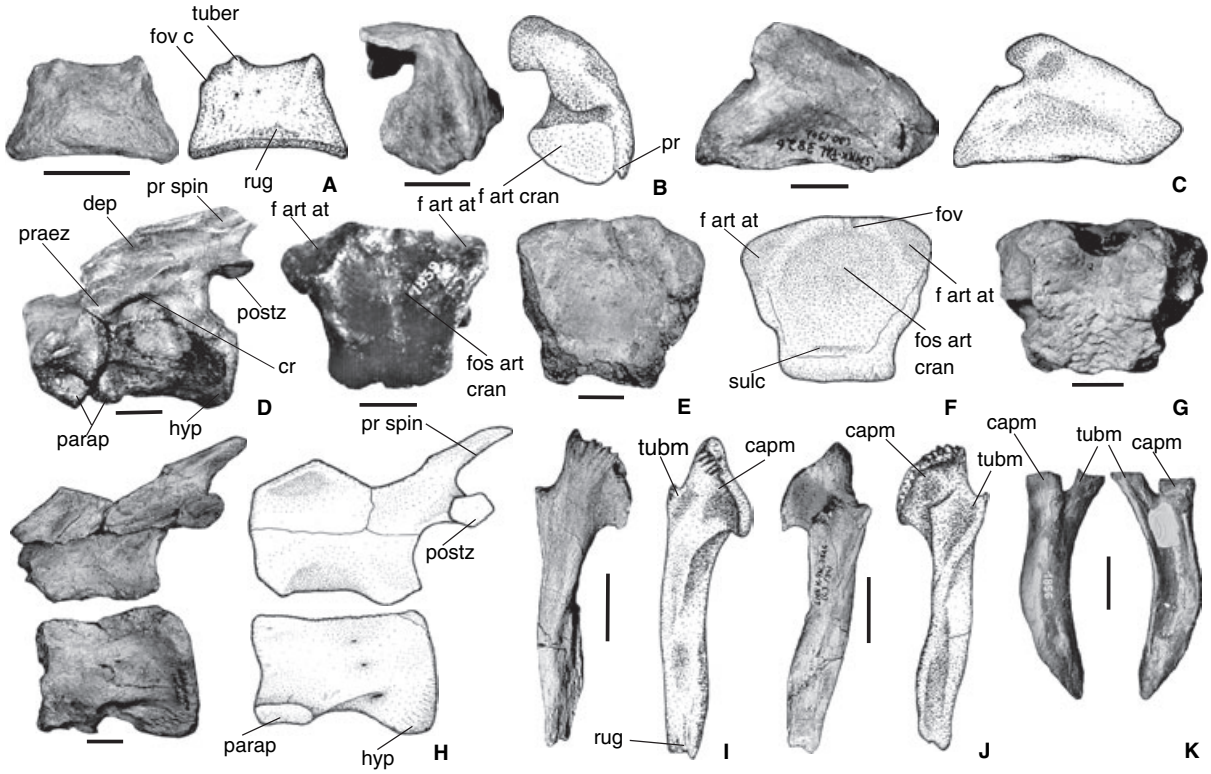

TEXT-FIG. 2. Photographs and drawings of cervical vertebrae and ribs of the Hyposaurinae. A, photograph (left) and drawing (right) of atlas intercentrum of *Dyrosaurus* sp. (SMNK-PAL 3826 28/94) in dorsal view. B–C, left arcuate element of the neural arch of the atlas of *Dyrosaurus* sp. (SMNK-PAL 3826 29/94). B, photograph (left) and drawing (right) in cranial view; C, photograph (left) and drawing (right) in lateral view. D, photograph of dens and axis of *Congosaurus bequaerti* (MRAC 1839 and 1879), lateral view. E, photograph of dens of *Congosaurus bequaerti* (MRAC 1839), cranial view. F–G, dens (SMNK-PAL 3826 31/94) of *Dyrosaurus* sp. F, photograph (left) and drawing (right) of cranial view; G, photograph of caudal view. H, photograph (left) and drawing (right) of axis of *Dyrosaurus* sp. (SMNK-PAL 3826 62/94) in lateral view. I–J, right axial rib of *Dyrosaurus* sp. (SMNK-PAL 3826 43/94). I, photograph (left) and drawing (right) of lateroventral view; J, photograph (left) and drawing (right) of mediodorsal view. K, photographs of left axial rib of *Congosaurus bequaerti* (MRAC 1856) in lateral (left) and medial (right) views. For abbreviations see text. Scale bars represent 20 mm.

the elastic ligament is a shallow, median, high-oval depression at the caudal margin of the neural arch of the axis at the base of the neural spine. The praezygapophysis of the axis is longitudinally oval and orientated dorsolaterally (Text-fig. 2D). It merges with the cranial margin of the neural arch of the axis. In contrast to extant crocodilians, the ventral margin of the praezygapophysis continues caudally as a ridge on the lateral surface of the neural arch of the axis. In the middle of the neural arch of the axis this ridge curves ventrally and merges with the ventral margin of the neural arch of the axis. Ventral to this ridge, a deep depression is visible (Text-fig. 2D, H). The articular surface of the postzygapophysis of the axis of *Dyrosaurus* (SMNK-PAL 3826 (62/94)) and *Congosaurus* (MRAC 1870) is directed craniomedially and forms an angle of approximately 30 degrees with the median plane, whereas in *Crocodylus porosus* this angle is 37 degrees (Text-fig. 3A). The neural spine of the axis of *Dyrosaurus* and *Congosaurus* is rodlike and points caudodorsally at an angle of 45 degrees to the horizontal (Text-fig. 2D, H), as in *Tomistoma schlegeli* (Hoffstetter and Gasc 1969). The height of the neural spine reaches three-quarters of the corpus length. The dorsal margin of the neural spine is transversally broadened and covered with lateromedially directed, delicate striae. In the caudal half of the neural spine a depression lies on either side, laterally adjacent to its dorsal margin.

Condylar fossa for the occipital condyle. The bowl-shaped condylar fossa for the occipital condyle is formed by the cranial surfaces of the dens (Text-fig. 2E–F), the atlas intercentrum and the cranial articular surfaces of the atlas neural arch (Text-fig. 2B).

Third–ninth cervical vertebrae. Dorsomedially in the cranial vertebral fossa of the cervical vertebrae of *Dyrosaurus* (SMNK 3826) a circular tubercle is developed, whereas dorsomedially in the caudal vertebral fossa of *Dyrosaurus* (SMNK 3826) and *Hyposaurus* (MNHN) a circular depression is present (Text-fig. 4A–B). In ventral aspect, the third–ninth cervicals of the Hyposaurinae are weakly hour-glass-shaped, with a width at the constriction that is two-thirds of the width at their caudal vertebral margin.

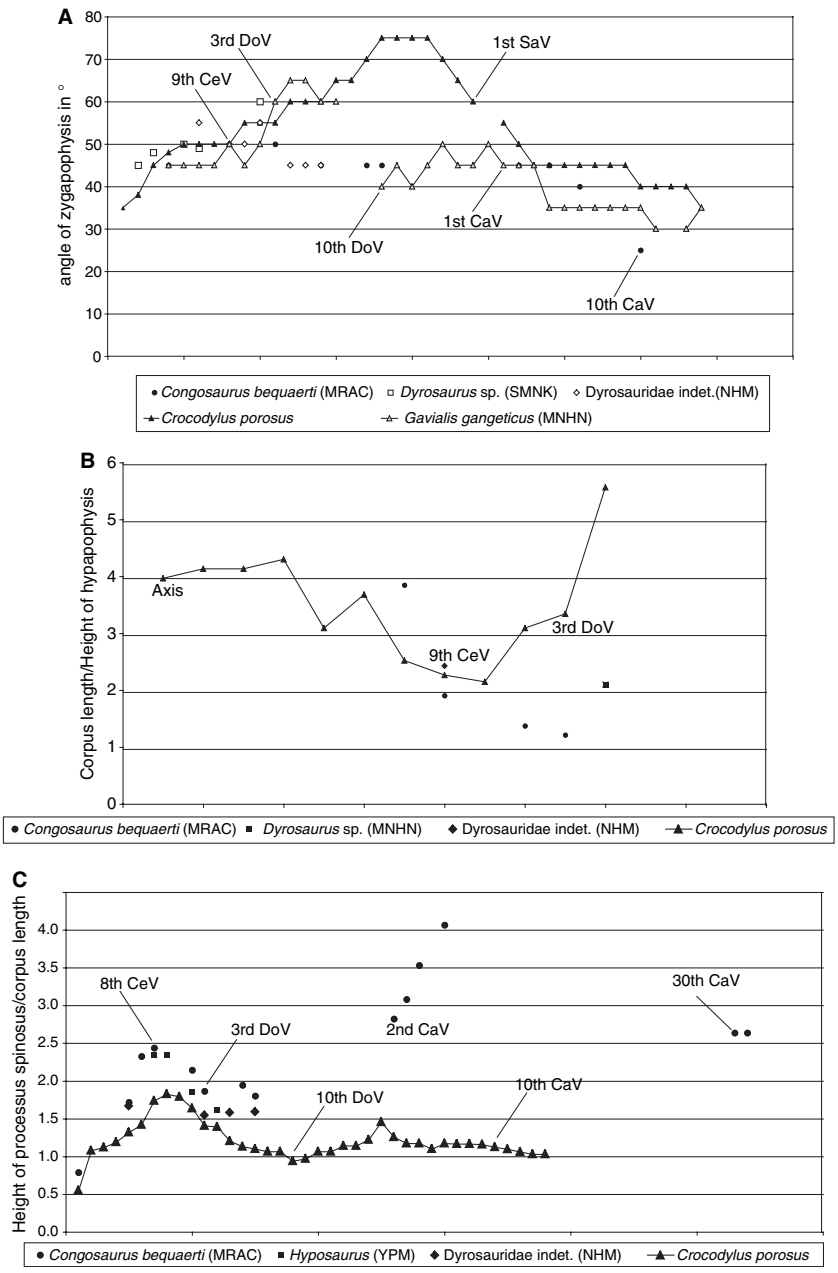

TEXT-FIG. 3. Comparison of proportions within the axial skeleton of the Hyposaurinae and recent crocodilians. A, angles of praezygapophyses to the median plane. B, heights of hypapophyses in relation to corpus length. C, heights of neural spines in relation to corpus length.

The hypapophyses of the third and fourth cervicals are similar to that of the axis (Text-fig. 4D). At the fifth cervical, the hypapophysis forms a strongly rugose tuberosity and the hypapophysis of the sixth cervical is reduced to a median crest along the ventral surface of the vertebral body (Text-fig. 4E; Langston 1995). The hypapophysis of the seventh cervical of *Dyrosaurus* [SMNK 3826 (53/94); Thevenin 1911, pl. 3, fig. 4a] and of cf. *Rhabdognathus* (Langston 1995) is hatchet-shaped and forms a caudally protruding, rounded crest, whereas in *Congosaurus* (Text-fig. 4G) and *Hyposaurus* (MNHN IF 16-2 Coll. Arambourg; Storrs 1986) it is a blunt median crest running over the entire length of the vertebral body. On the eighth cervical, the hypapophysis of *Dyrosaurus* is twice as high as that of *Congosaurus* (Text-fig. 4I) with respect to the length of the vertebral body. In all Hyposaurinae examined, the hypapophysis of the ninth cervical is half as high as the vertebral body is long (Text-fig. 3B). In contrast, the hypapophyses of the third–sixth cervical vertebra of *Crocodylus porosus* are distinct processes that are positioned in the rostral third of the ventral surface of the vertebral body (Text-fig. 3B).

The bodies of the cervical vertebrae are maximally twice as long as they are high and are laterally concave. In lateral aspect, the bodies of the cervical vertebrae are ventrally one-tenth longer than dorsally (Text-fig. 4; Troxell 1925; Norell and Storrs 1989; Langston 1995). The neurocentral suture is ventrally convex (Pomel 1894; Thevenin 1911; Langston 1995).

The parapophyses of the third–sixth cervical vertebrae emerge from the cranioventral surface of the vertebral body. In *Dyrosaurus* and *Congosaurus*, the parapophyses are located dorsomedially at the seventh and eighth cervicals, and positioned adjacent to the neurocentral suture at the ninth cervical (Text-fig. 4G, I). The parapophyses of cf. *Rhabdognathus* emerge from the middle of the lateral surface of the sixth–ninth cervical of the vertebral body (Langston 1995). The diapophysis of the third cervical of *Dyrosaurus* and *Congosaurus* lies over the neurocentral suture and only its ventral third is formed by the vertebral body (Fig. 4D). From the fourth cervical caudally, the diapophyses of *Congosaurus* emerge from the neural arch, whereas the diapophyses of *Dyrosaurus* are gradually displaced dorsally from the fourth to the seventh cervical (Text-fig. 4C, E, G–H). In cf. *Rhabdognathus* the ventral half of the diapophysis is formed by the vertebral body whereas its dorsal half is formed by the neural arch (Langston 1995). In comparison, the parapophyses of the cervicals of *Crocodylus porosus* are positioned at the cranial margin of the lateral surface of the vertebral body and the diapophyses are formed exclusively by the neural arch.

The peduncle of the neural arch of the cervical vertebrae of the Hyposaurinae is approximately one-fifth lower than that of *Crocodylus porosus* and in contrast to the latter, becomes even lower between the seventh and the ninth cervicals. An area for the elastic ligament is developed as a deep, median high-oval fovea between the prae- and postzygapophyses, respectively. This ligament area becomes higher at the eighth and ninth cervical (Text-fig. 4F, H). The angle of the articular surfaces of the prae- and postzygapophyses to the median plane is approximately 45 degrees in the cranial cervical region and increases to approximately 50 degrees in the caudal cervical region (Text-fig. 3A; Hua 2003).

The height of the neural spine of the third cervical vertebra of *Congosaurus* (MRAC 1840; Jouve and Schwarz 2004) and *Hyposaurus* (Troxell 1925) reaches 1·2 times the length of the vertebral body. From the fourth to the ninth cervical, the height of the neural spines increases to 2·1 times the length of the vertebral body in *Dyrosaurus* (Arambourg 1952) and *Hyposaurus* (YPM 17827; Troxell 1925) and to 2·4 times the length of the vertebral body in *Congosaurus* (Text-fig. 3C). In comparison, the neural spine of the ninth cervical of *Crocodylus porosus* reaches 1·8 times the length of the vertebral body (Text-fig. 3C).

The neural spine of the third cervical vertebra is directed caudodorsally, in *Congosaurus* at an angle of 40 degrees to the horizontal plane (Text-fig. 4D) and in *Dyrosaurus* at an angle of 45 degrees. The dorsal third of the neural spine forms a rod with an almost circular cross-section. The neural spines of the fourth–ninth cervicals point straight dorsally (Troxell 1925; Arambourg 1952) and possess a vaulted dorsal margin which is three-quarters of their basal length (Text-fig. 4E). The neural spine of the seventh cervical gently bends caudodorsally and decreases by one-sixth from its basal length to its convex dorsal margin (Text-fig. 4G). The neural spines of the eighth and ninth cervicals are slightly caudally inclined and show a convex dorsal margin that has only one-third of its basal length in the eighth cervical (Text-fig. 4I).

Cervical ribs. The presence of a fovea for the first cervical rib at the lateral surface of the atlas intercentrum (Text-fig. 2A) indicates the presence of a single-headed atlas rib in the Hyposaurinae, though the rib itself is not preserved. The axis rib is 1·5 times the length of the axial body and overlaps the cranial third of the third cervical rib (Text-fig. 5A). The corpus of the axis rib is longitudinally directed and cranially bifurcates into capitulum and tuberculum (Text-fig. 2I–K). The body of the third–seventh cervical ribs is orientated craniocaudally with the capitulum and tuberculum directed perpendicular to the costal body in a medial direction. The third and fourth cervical ribs are one-quarter and the fifth–seventh cervical ribs are one-fifth longer than the adjacent vertebral bodies, whereas in *Crocodylus porosus*, the third–seventh cervical ribs exceed the length of the adjacent vertebral body by one-third (Text-fig. 5A). The medial surface of the body of the third and fourth cervical ribs is two-thirds lower than its lateral surface and the internal surface of the rib forms a concave trough (Text-fig. 4K). The cranial process and the caudal quarter of the body of the third–seventh cervical ribs each bear a lateral and a medial rugosity, which are most prominent on the third and fourth cervical ribs (Text-fig. 4J–K, M–O).

The eighth and ninth cervical ribs of *Dyrosaurus* (SMNK 3826), *Congosaurus* (Text-fig. 4L) and *Hyposaurus* (Troxell 1925; Storrs 1986) are orientated in a vertical plane. The eighth cervical rib of *Congosaurus* is one-tenth longer and that of *Dyrosaurus* is two-thirds longer than the adjacent vertebral body (Text-fig. 5A). The eighth cervical rib of *Congosaurus* possesses a distinct cranial process and a strongly rugose ventral margin (Text-fig. 4L).

Dorsal vertebrae. In ventral view, the bodies of the dorsal vertebrae are hour-glass-shaped. Their width at the constriction is two-thirds their width at the caudal margin. In lateral aspect, the first–eighth dorsal vertebral bodies of the Hyposaurinae are one-third longer than high; those of the caudal dorsals are two-thirds longer than high (Text-fig. 6A–C, F–G). The dorsal vertebral bodies are five per cent shorter at the ventral margin than at the neurocentral suture (Troxell 1925; Norell and Storrs 1989; Langston 1995).

The cranial vertebral fossa of the dorsal vertebrae of *Congosaurus* bears a dorsomedially positioned circular tuber. In *Dyrosaurus* and *Congosaurus* the caudal vertebral fossa bears a dorsomedial circular depression. The caudal surface of the first praesacral vertebra of *Dyrosaurus* is kidney-shaped with a transversely orientated long axis. The caudal surface of the last praesacral vertebra is rugose and its lateral third forms an articular surface for the first sacral rib (Text-fig. 6E).

The lateral surfaces of the bodies of the dorsal vertebrae of *Dyrosaurus* (SMNK, MNHN) converge slightly and those of *Congosaurus* (Jouve and Schwarz 2004), *Hyposaurus* (YPM; Arambourg 1952) and cf. *Rhabdognathus* (Langston 1995) converge strongly in a ventral direction. The hypapophyses of the first–third dorsal vertebrae are straight, ventrally directed and as high as the vertebral body (Text-figs 3B, 6A–C). The hypapophysis of the fourth dorsal vertebra bends caudally and is half as high as the vertebral body. The hypapophysis of the fifth dorsal forms a hatchet-shaped process in the cranial half of the ventral surface of the vertebral body. The ventral surface of the sixth dorsal vertebra of the Hyposaurinae bears a median crest. In *Congosaurus,* this crest is present in all caudally following dorsal

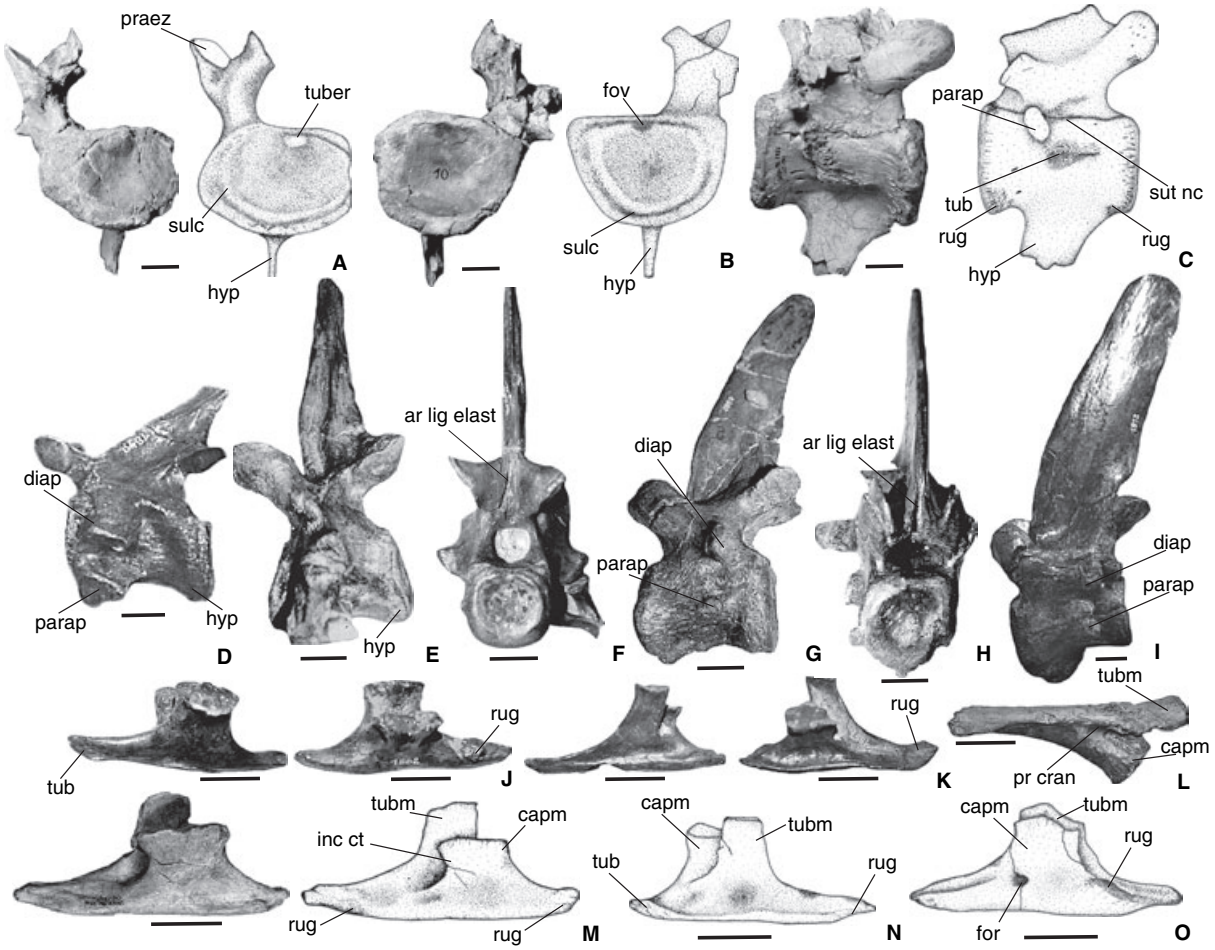

TEXT-FIG. 4. Photographs and drawings of cervical vertebrae and ribs of the Hyposaurinae. A–C, ninth cervical vertebra of *Dyrosaurus* sp. (SMNK-PAL 3826 55/94). A, photograph (left) and drawing (right) in cranial view; B, photograph (left) and drawing (right) in caudal view; C, photograph (left) and drawing (right) in lateral view. D–L, photographs of cervical vertebrae and ribs of *Congosaurus bequaerti*. D, third cervical vertebra (MRAC 1840), lateral view. E–F, sixth cervical vertebra (MRAC 1871). E, lateral view; F, caudal view. G–H, seventh cervical vertebra (MRAC 1869). G, lateral view; H, cranial view. I, eighth cervical vertebra (MRAC 1872), lateral view. J, right fifth cervical rib (MRAC 1862), lateral (left) and medial (right) views. K, right third cervical rib (MRAC 1864), lateral (left) and medial (right) views. L, left eighth cervical rib (MRAC 1789), lateral view. M–O, cervical ribs of *Dyrosaurus* sp. M, photograph (left) and drawing (right) of left third cervical rib (SMNK-PAL 3826 42/94), medial view; N, drawing of lateral view. O, drawing of left fourth cervical rib (SMNK-PAL 3826 37/94), medial view. For abbreviations, see text. Scale bars represent 20 mm.

vertebrae. In *Crocodylus porosus*, the caudalmost hypapophysis is developed on the third dorsal vertebra. The longitudinally straight neurocentral suture of the dorsal vertebrae of the Hyposaurinae is entirely unfused.

The parapophysis and the diapophysis contact each other at the third dorsal vertebra. A transverse process, bearing parapophysis and diapophysis, is developed in *Dyrosaurus*, *Congosaurus* and *Hyposaurus* from the fourth dorsal vertebra onwards and in cf. *Rhabdognathus* (Langston 1995) from the fifth dorsal vertebra onwards. The transverse processes protrude from the lateral surface of the neural arch laterally (Text-fig. 6D–E). Ventrally at the bases of the transverse processes of *Dyrosaurus* (SMNK-PAL 3826) and *Congosaurus* (Jouve and Schwarz 2004) lies a ventral depression. Owing to their poor preservation, the widths of the transverse processes in the trunk can only be calculated by correlation with their length. The length of the transverse processes increases continuously from cranial to caudal as does the length-width ratio of the transverse processes (Text-fig. 5B–C). The width of the transverse processes increases between the fourth and seventh dorsal vertebrae, and decreases in a caudal direction to the tenth dorsal vertebra. In contrast to *Crocodylus porosus*, the width of the transverse processes of the Hyposaurinae does not exceed the length of the vertebral body (Text-figs 5B–C, 6I), but the transverse processes in relation to the length of the vertebral body are longer than in *Crocodylus porosus*.

The area for the elastic ligament of the dorsal vertebrae forms a deep vertical sulcus (Text-fig. 6D–E), which covers the ventral half of the cranial margin and the ventral two-thirds of the caudal margin of the neural spine. The articular surfaces of the

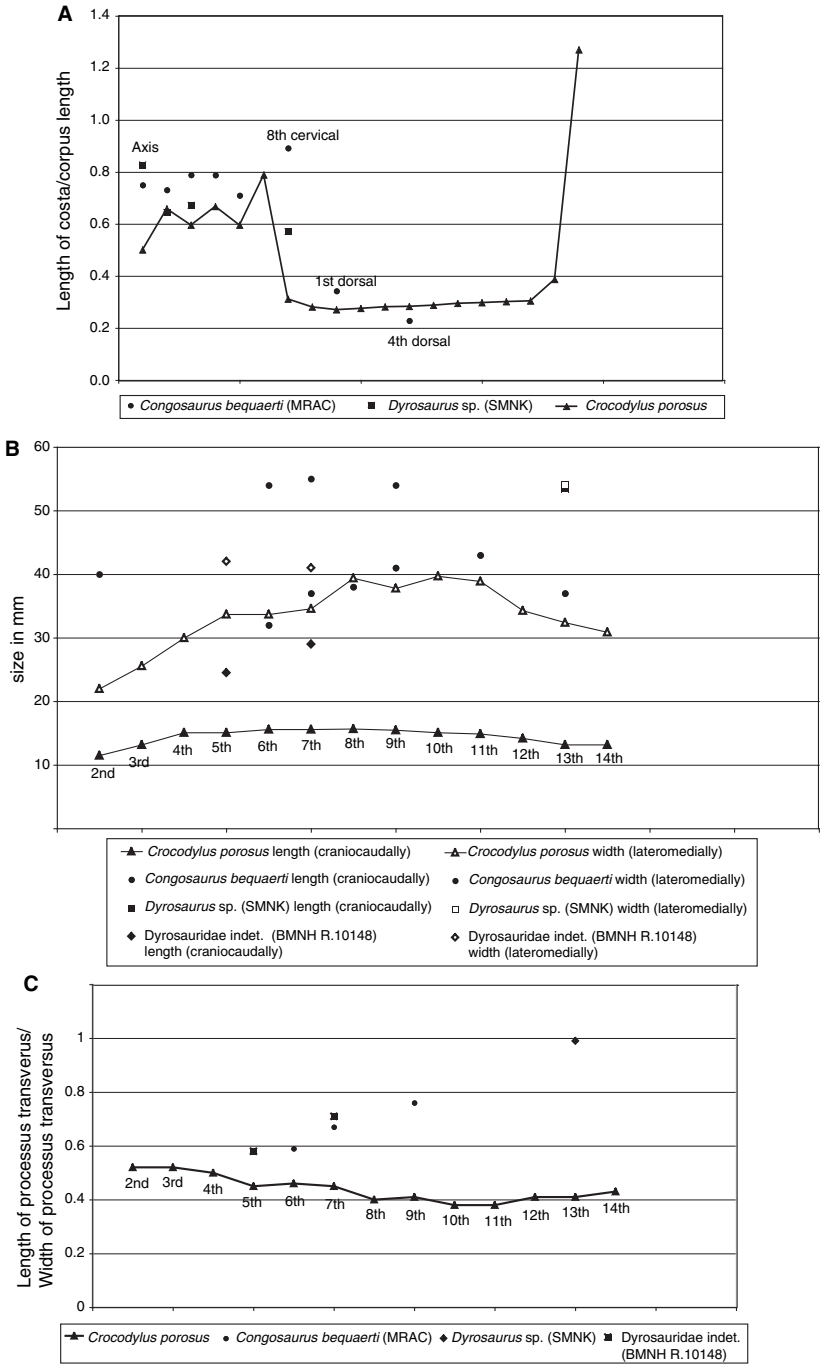

TEXT-FIG. 5. Comparison of proportions within the axial skeleton of the Hyposaurinae and *Crocodylus porosus*. A, relationship between the length of the ribs and the adjacent vertebral bodies. B, length and width of the transverse processes (numbers in diagram indicate corresponding dorsal vertebra). C, relationship between length and width of the transverse processes (numbers in diagram indicate corresponding dorsal vertebra).

prae- and postzygapophyses of the first–third dorsal vertebrae of *Congosaurus*, *Dyrosaurus*, *Hyposaurus* and an undetermined dyrosaurid crocodilian (BMNH 10148) are inclined medioventrally at 50 degrees to the median plane, which is also the case in the extant crocodilians *Crocodylus porosus* and *Gavialis gangeticus* (Text-fig. 3A). At the fourth–thirteenth dorsal vertebrae, the articular surfaces of the prae- and postzygapophyses of *Congosaurus*, *Dyrosaurus*, *Hyposaurus* and an undetermined dyrosaurid crocodilian (BMNH 10148) form angles of 45–50 degrees with the median plane, and are therefore steeper than in *Crocodylus porosus* (Text-fig. 3A).

The neural spines decrease in height between the first and fourth dorsal vertebrae and have similar heights between the fourth and fourteenth dorsal vertebra (Text-fig. 3C). In *Congosaurus* (Text-fig. 6C; Jouve and Schwarz 2004) and in the neural spine of the fifteenth dorsal vertebra of cf. *Rhabdognathus* (Langston 1995), the height of the neural spines is 1·8 times the length of the vertebral body. In *Hyposaurus* (YPM 17827; Troxell 1925; Storrs 1986), the height of the neural spines is 1·4 times the length of the vertebral body. The neural spines of some dorsal vertebrae of the medial part of the truncus of an undetermined dyrosaurid crocodilian

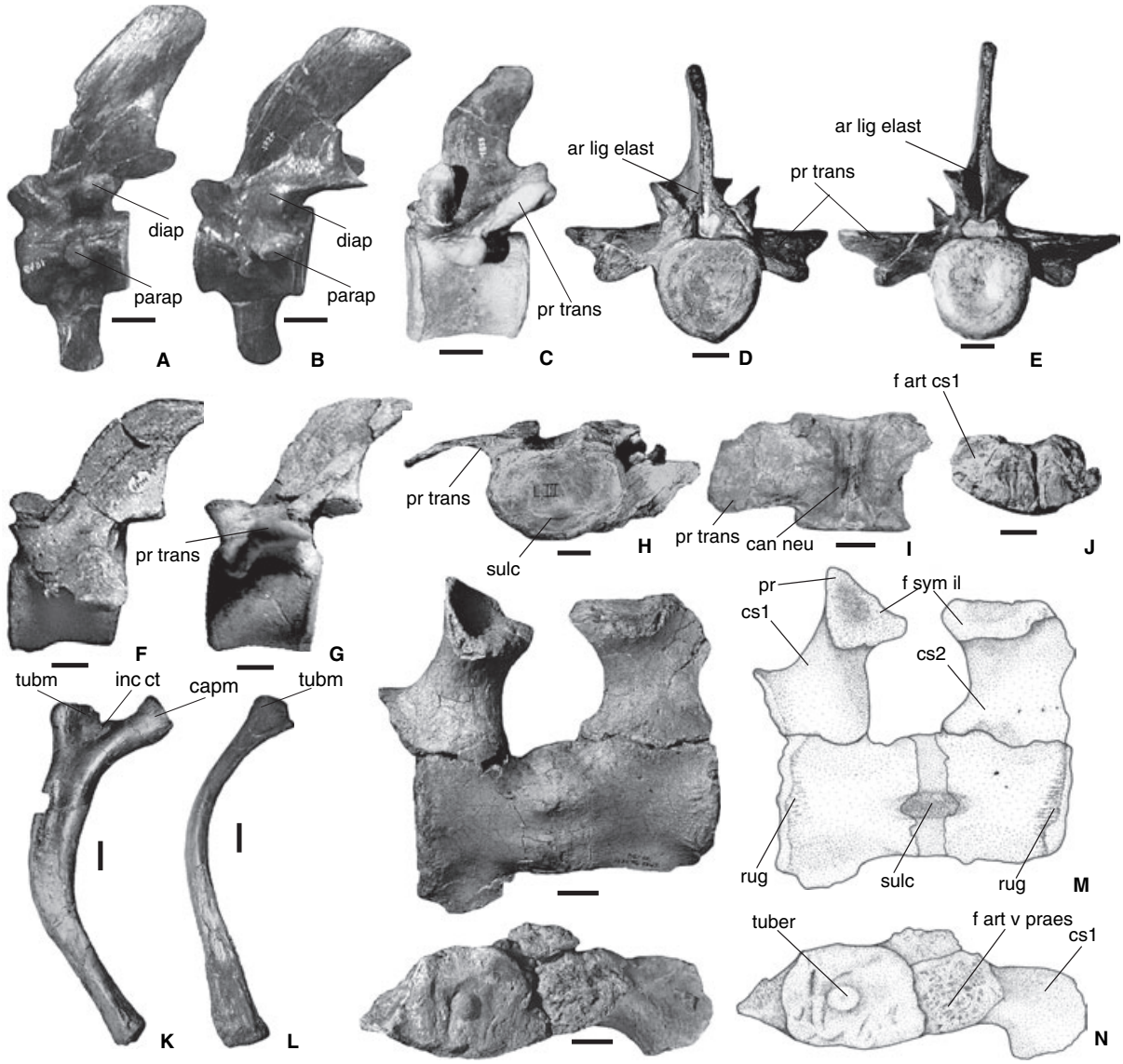

TEXT-FIG. 6. Photographs and drawings of dorsal and sacral vertebrae and ribs of the Hyposaurinae. A–G, photographs of dorsal vertebrae of *Congosaurus bequaerti*. A, second dorsal vertebra (MRAC 1849), lateral view. B, third dorsal vertebra (MRAC 1854), lateral view. C–E, seventh dorsal vertebra (MRAC 1855). C, left lateral view; D, cranial view; E, caudal view. F, photograph of seventh dorsal vertebra of an undetermined dyrosaurid crocodilian (BMNH R. 10148), lateral view. G, photograph of eighth dorsal vertebra of an undetermined dyrosaurid crocodilian (BMNH R. 10148), lateral view. H–I, photographs of caudal dorsal vertebra of *Dyrosaurus* sp. (SMNK-PAL 3826-71/94). H, cranial view; I, dorsal view. J, photograph of first praesacral vertebra of *Dyrosaurus* sp. (SMNK-PAL 3826-70/94) in caudal view. K–L photographs of thoracic ribs of *Congosaurus bequaerti* in external (lateral) view. K, MRAC (1745); L, MRAC (1743). M–N, first and second sacral vertebrae and ribs of *Dyrosaurus* sp. (SMNK-PAL 3826 69/94). M, photograph (left) and drawing (right) in ventral view; N, photograph (left) and drawing (right) in cranial view. For abbreviations, see text. Scale bars represent 20 mm.

(BMNH No. R.10148) are 1·6 times as high as the vertebral body is long (Text-fig. 6F–G).

The dorsal neural spines are approximately 1·6 times higher than the length of the vertebral bodies and the lumbar and sacral neural spines increase in height in new specimens of *Dyrosaurus* spp. from Morocco (S. Jouve, pers. comm. 2002). In *Crocodylus porosus*, however, the neural spines of the dorsal vertebrae are 1·1 times as high as the vertebral body is long and in the base of the tail reach a maximum of 1·4 times as high (Text-fig. 3C).

In lateral view, the dorsal quarter of the neural spines of the first–seventh dorsal vertebrae bends caudodorsally (Text-fig. 6C, F–G). The dorsal margin is convex and forms a wide curve to the cranial margin (Langston 1995; Jouve and Schwarz 2004). The neural spines of the ninth–fourteenth dorsal vertebra are straight and dorsally directed (Langston 1995) and possess a

weakly convex dorsal margin that is laterally broadened and laterally rugose.

Thoracic ribs. The first, second and fourth thoracic ribs are preserved in the partial skeleton of *Congosaurus bequaerti* (MRAC; Jouve and Schwarz 2004). The partial skeleton of cf. *Hyposaurus* (Storrs 1986) bears 17 thoracic ribs that are preserved in closest proximity to the vertebral column, but are not articulated. An incomplete thoracic rib together with its adjacent vertebral body is preserved in *Hyposaurus* (YPM 17827). The number of thoracic ribs in the Hyposaurinae is at least ten.

The first thoracic rib (MRAC 1745) of *Congosaurus* is three times as long as the adjacent vertebral body, and the second thoracic rib (MRAC 1743) of *Congosaurus* is five times as long. The thoracic ribs of *Hyposaurus* (YPM 17827; Storrs 1986) are at least 5·5 times as long as the vertebral bodies whereas in *Crocodylus porosus* the thoracic ribs are at most three times as long as the vertebral bodies (Text-fig. 5A). In the postcranial skeletons of yet undescribed remains of *Dyrosaurus* spp. from Morocco (S. Jouve, pers. comm. 2002) only the two or three caudalmost thoracic ribs decrease in length.

The costal body is strongly curved dorsally in its dorsal half, with a highly convex cranial and a deeply concave caudal margin (Text-fig. 6K–L). In its ventral half, the costal body is straight and ventrally directed. The ventral third of the body of the first and second thoracic ribs of *Congosaurus* is broadened and bears a median crest on its lateral surface. Where present, the capitulotubercular concavity is semicircular. Flat, blade-like lateral costal segments of cf. *Rhabdognathus* were described by Langston (1995). These lateral segments widen proximally and form articular surfaces for the vertebral rib segments. These surfaces possess a rugose, pitted surface (Langston 1995).

Gastral ribs. Langston (1995) described the lateral segment of a caudalmost gastral rib of cf. *Rhabdognathus*. A pathological gastral rib with a callus is present in the partial skeleton of *Congosaurus bequaerti* (MRAC 1747). This rib is slightly convex laterally and circular in cross-section.

Sacrum. The rugose cranial surface of the first sacral vertebra is irregularily pentagonal in outline and contacts with its lateral quarters the first pair of sacral ribs (Text-fig. 6N). In *Dyrosaurus* and *Hyposaurus* (YPM 753), the cranial surface of the first sacral vertebra bears a circular tuber centrally (Text-fig. 6N). The caudal surface of the second sacral vertebra of *Dyrosaurus phosphaticus* (Arambourg 1952) and *Hyposaurus* (YPM 753) bears two parallel, dorsoventrally orientated sulci. In *Dyrosaurus* sp. (SMNK-PAL 3826), the second sacral ribs only contact laterally the caudal surface of the second sacral vertebra, whereas in cf. *Rhabdognathus* they form the lateral third of the caudal vertebral surface (Langston 1995). The ventral surfaces of the first sacral vertebra of *Dyrosaurus* sp. and cf. *Rhabdognathus* bear a shallow median sulcus (Text-fig. 6M). The vertebral bodies of the first and second sacral vertebrae are fused in the partial skeleton of *Dyrosaurus* sp. (SMNK-PAL 3826, Text-fig. 6M) and connected by a serrated suture in *Hyposaurus* (YPM 753). The neural spines of the two sacral vertebrae of yet undescribed material of *Dyrosaurus* spp. from Morocco are similar in outline to those of the caudal dorsal vertebrae and as high as the neural spines of the second dorsal vertebra (S. Jouve, pers. comm. 2002).

The first sacral rib of *Dyrosaurus* sp. (SMNK-Pal 3826) is one-third wider than the transverse process of the second praesacral vertebra, whereas the second sacral rib reaches four-fifths the width of the first sacral rib. The first and second sacral rib are hour-glass-shaped in ventral view (Text-fig. 6M). The iliac symphysial surface of the first sacral rib of *Dyrosaurus* (SMNK-PAL 3826) and cf. *Rhabdognathus* (Langston 1995) is square with rounded corners and possesses a craniolateral process that does not occur in *Crocodylus porosus* (Text-fig. 6M). The second sacral rib of cf. *Rhabdognathus* (Langston 1995) possesses an iliac symphysial surface that is cranially convex and forms a caudodorsally directed process that exceeds the body of the second sacral vertebra for two-thirds of its length.

Caudal vertebrae. The bodies of the caudal vertebrae have a shallow bowl-shaped cranial and caudal vertebral fossa (Text-fig. 7D–F). After the ninth caudal vertebra the vertebral fossae are reduced to shallow median depressions. The length of the caudal vertebral bodies decreases from the third caudal vertebra to the tip of the tail, whereas in *Crocodylus porosus* the length of the vertebral bodies decreases only from the fifteenth caudal vertebra. The first–fourth vertebral bodies are 1·3 times as long as they are high and, in relation to their height, increase in length more than twice at the fourteenth caudal vertebra.

In ventral view, the bodies of the caudal vertebrae are weakly hour-glass-shaped with a width at the constriction that is three-quarters of the width at their caudal vertebral margin (Text-fig. 7B). The cranial articular surface for the haemal arch has an angle of 40 degrees and the terminal articular surface for the haemal arch has an angle of 60 degrees in caudal and cranial directions to the horizontal plane, respectively. In the partial skeletons of *Dyrosaurus* sp. (SMNK 3826) and cf. *Rhabdognathus* (Langston 1995) the cranialmost articular surface for the haemal arch is developed at the second caudal vertebra. In the partial skeleton of *Congosaurus bequaerti* (MRAC; Jouve and Schwarz 2004) the cranialmost articular surface for the haemal arch is developed at the third caudal vertebra.

In lateral view, the ventral margin of the bodies of the caudal vertebrae is concave (Text-fig. 7C, G–J, M). The lateral surface of the bodies of the first–seventh caudal vertebrae is weakly concave, and that of the terminally adjacent ones is deeply concave. The neurocentral suture is slightly convex ventrally on the first caudal vertebra of *Dyrosaurus* sp. (SMNK 3826) and weakly convex dorsally on the following terminal caudal vertebrae of *Dyrosaurus* sp. (Text-fig. 7A, SMNK-PAL 3826 68/94) and *Congosaurus* (Jouve and Schwarz 2004). The terminal caudal vertebrae bear a rugose crest on the lateral vertebral surface where the neurocentral suture should be.

In dorsal view, the first–fourth caudal ribs of the Hyposaurinae curve caudally (Text-fig. 7A–D). The costal process tapers from medial to lateral to three-quarters of its craniocaudal length at the base. The second caudal rib is as wide as the second sacral rib. The third caudal rib is as wide as the first caudal rib, the lateral extension of which is 16 per cent shorter than the second caudal rib in the Hyposaurinae and 4 per cent in *Crocodylus porosus* (Text-fig. 8). At least the fifth–tenth caudal vertebrae of the

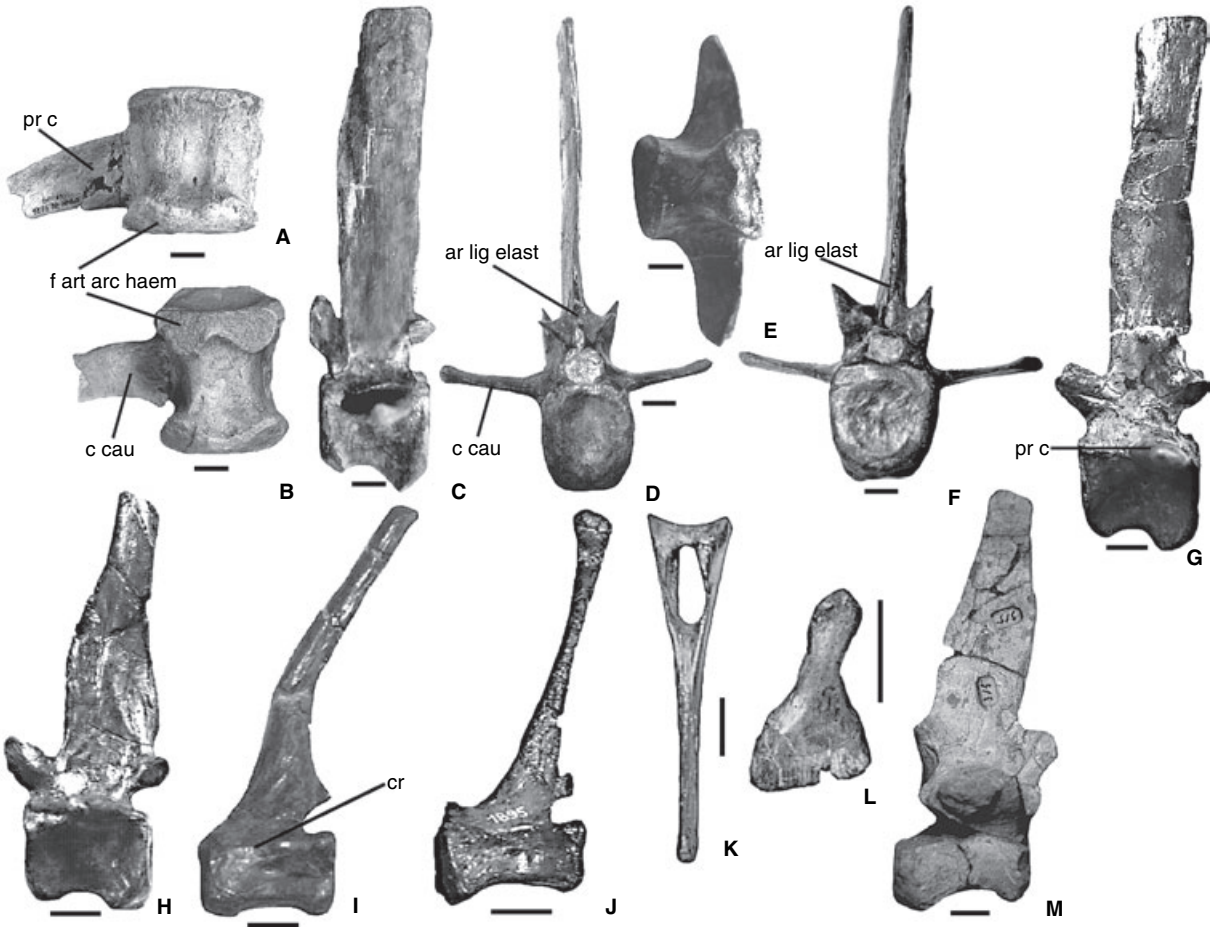

TEXT-FIG. 7. Photographs of caudal vertebrae of the Hyposaurinae. A, second caudal vertebra of *Dyrosaurus* sp. (SMNK-PAL 3826 68/94) in ventral view. B, third caudal vertebra of *Dyrosaurus* sp. (SMNK-PAL 3826 67/94) in ventral view. C–L, caudal vertebrae of *Congosaurus bequaerti*. C–F, fourth caudal vertebra (MRAC 1888). C, lateral view; D, cranial view; E, ventral view; F, caudal view. G, sixth caudal vertebra (MRAC 1852), lateral view. H, ninth caudal vertebra (MRAC 1892), lateral view. I, twenty-seventh caudal vertebra (MRAC 1893), lateral view. J, thirty-first caudal vertebra (MRAC 1895), lateral view. K, haemal arch from the tail base (MRAC 1877), cranial view. L, haemal arch from the medial region of the tail (MRAC 1881), lateral view. M, seventh caudal vertebra of *Hyposaurus derbianus* (BMNH no. 315), lateral view. Scale bars represent 20 mm.

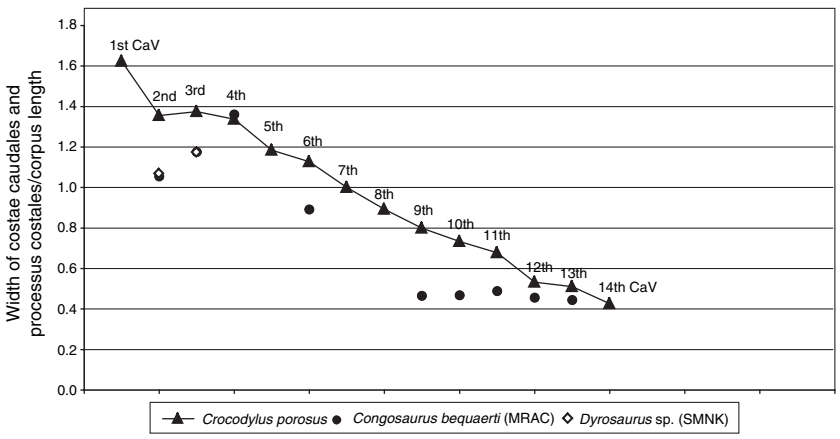

TEXT-FIG. 8. Relationship between width of caudal ribs/costal processes and the adjacent vertebral bodies in the Hyposaurinae and *Crocodylus porosus* (numbers in diagram indicate corresponding caudal vertebra).

Hyposaurinae possess costal processes that bend cranially (Text-fig. 7G). In comparison with the length of the adjacent vertebral bodies, the costal processes of the Hyposaurinae are one-quarter shorter than in *Crocodylus porosus* (Text-fig. 8).

The area for the elastic ligament of the first–eighth caudal vertebrae forms a median fovea that continues dorsally from the zygapophyses as a thin median groove over the ventral quarter of each neural spine (Text-fig. 7C, F). Between the ninth and twentieth caudal vertebrae the area for the elastic ligament gradually decreases in height; the terminal caudal vertebrae lacking costal processes possess only a small, rugose area for the elastic ligament. The roof of the neural arch of the cranialmost caudal vertebrae is slightly convex, but on the medial and terminal ones it is vaulted successively higher. The zygapophyses of the first–tenth caudal vertebrae of the Hyposaurinae bear articular surfaces that have angles five degrees steeper to the median plane than *Crocodylus porosus*, and angles five degrees shallower than in *Gavialis gangeticus* (Text-fig. 3A). From the eleventh caudal vertebra onwards the zygapophyses are reduced to short, rod-like, longitudinally orientated processes.

The height of the neural spines increases from the first to the sixth caudal vertebra, where it reaches more than four times the length of the vertebral body (Text-fig. 3C). Between the seventh and twentieth caudal vertebrae the height of the neural spines decreases to about one-tenth. The neural spine of the thirty-first caudal vertebra of *Congosaurus bequaerti* (MRAC 1895) is still half as high as the neural spine of the sixth caudal vertebra, which is the highest in the series. In *Crocodylus porosus*, the highest neural spine of the tail is at the second caudal vertebra and is 1·4 times as high as the vertebral body is long (Text-fig. 3C).

The neural spines of the first–sixth caudal vertebrae of the Hyposaurinae are straight and dorsally directed (Swinton 1950; Langston 1995) with a slightly vaulted and rugose dorsal margin (Text-fig. 7C, G). The neural spines of the seventh–twentieth caudal vertebrae are constricted dorsally to their base, but become longitudinally expanded in their dorsal third (see also reconstruction in Text-fig. 1C). The dorsal margins of the neural spines are convex and broadened (Text-fig. 7H, M). From the thirty-first caudal vertebra terminally, the neural spines are caudally inclined at an angle of 70 degrees to the horizontal plane (Text-fig. 7I–J). These terminal neural spines possess a rod-shaped shaft with a rostroterminally oval cross-section that increases to twice its ventral length in its dorsal quarter. The dorsal margin of these neural spines is straight, transversely broadened and laterally rugose.

Haemal arches. The second haemal arch of *Congosaurus bequaerti* (MRAC 1876) and cf. *Rhabdognathus* (Langston 1995) between the third and fourth caudal vertebrae is 3·4 times longer than the fourth caudal vertebral body is long (Text-fig. 7K). In cf. *Hyposaurus* (Storrs 1986), the first ten haemal arches are preserved and their height decreases between the third and the tenth to less than a half. In contrast, in *Crocodylus porosus*, the second haemal arch is one-third higher than the vertebral body is long and the height of the tenth haemal arch reaches two-fifths of the height of the third haemal arch. From the twelfth caudal vertebra terminally, the haemal arches of the Hyposaurinae are spatulate in lateral view (Text-fig. 7L). The right and left articular surfaces of the haemal arch are fused medially in *Congosaurus* (Jouve and Schwarz 2004) but are separate in cf. *Rhabdognathus* (Langston 1995).

Appendicular skeleton

Scapula. The scapula of the Hyposaurinae is one-third higher than the medially following neural spine of the eighth cervical vertebra. The scapular wing is longitudinally spatulate and as long as 3·5 vertebral segments (Text-fig. 9A–B), whereas the scapular wing of *Crocodylus porosus* is only as long as one vertebral segment. The cranial margin of the scapula of the Hyposaurinae is strongly concave, the caudal margin only slightly so (Text-fig. 9A–B). The ventral margin forms a strongly rugose coracoidal articular surface. The scapular part of the glenoid fossa faces caudoventrally (Troxell 1925; Langston 1995). Dorsally adjacent to the scapular part of the glenoid fossa a caudal tuberosity lies at the caudal margin of the scapular head (Text-fig. 9A). In lateral view, a bulging vertical cranial scapular process ('acromion process', Crush 1984) divides the cranial third from the caudal two-thirds of the lateral surface of the scapular head (Text-Fig. 10A). Cranially adjacent to the cranial scapular crest lies a prominent tuberosity. The lateral surface of the scapular head is rugose caudally to the crest.

Coracoid. The coracoid of the Hyposaurinae reaches four-fifths of the height of the scapula, whereas in *Crocodylus porosus* the scapula and coracoid are equally high. The coracoidal neck of the Hyposaurinae is rod-like and with a circular cross-section (Text-fig. 9C–E). The medially directed coracoidal wing is hatchet-shaped and reaches one-third of the length of the scapular wing (Text-fig. 9C–E; Troxell 1925; Langston 1995), whereas in *Crocodylus porosus* it is of equal length. The strongly rugose scapular articular surface forms the caudodorsal two-thirds of the dorsal margin of the coracoid. The coracoidal part of the glenoid fossa is rectangular with rounded corners and positioned on the caudoventrally projecting glenoid process (Langston 1995). The coracoidal head is perforated by a craniodorsally positioned, dorsoventrally oval, coracoidal foramen. Caudoventral to the glenoid process lies a caudal rugosity (Text-fig. 6D). A caudomedial tuberosity is cranially adjacent to the glenoid process on the medial surface of the coracoidal head. The lateral surface of the coracoidal head bears a ventrolateral rugosity at its cranial margin (Text-fig. 9C–D). In articulation, the long axes of the scapula and the coracoid of the Dyrosauridae form an angle of 125 degrees and the coracoid is ventromedially directed (Langston 1995, fig. F23B). The glenoid fossa is hour-glass-shaped in outline and ventrolaterally open (Langston 1995, fig. F23C).

Humerus. The humerus of the partial skeletons of *Congosaurus bequaerti* (MRAC 1813; Jouve and Schwarz 2004) and *Hyposaurus* (YPM 764; Troxell 1925) reaches 90 per cent of the length of the femur. The forelimbs of *Congosaurus* and *Hyposaurus* reach 90 per cent of the length of the hind limbs.

The humerus of the Hyposaurinae is straight (Text-fig. 9F–H; Bergounioux 1956; Langston 1995). The proximal extremity of the humerus is one-third wider than the humeral shaft (Text-fig. 9F–G). The humeral head of the Hyposaurinae bears a median, semi-spheroidal tuber, lateral to which the dorsal margin of the head is straight (Text-fig. 9F). In contrast, recent crocodilians such as *Crocodylus porosus* lack a tuber at the humeral head.

The deltopectoral crest, which arises from the proximal extremity of the medial surface of the humerus and runs parallel to its cranial surface, is blunt and oval in outline (Text-fig. 9G–H; Troxell 1925; Bergounioux 1956; Langston 1995). The deltopectoral crest terminates in a craniomedial tuberosity. In the medial third of its length, the deltopectoral crest is caudally accompanied by a rugosity. The craniolateral surface of the proximal extremity is strongly rugose. A sharp craniolateral ridge running from the distal end of the humeral head to the distal end of the proximal humeral extremity separates the craniolateral surface from the caudolateral surface of the proximal extremity (Text-fig. 9F). Between the craniolateral ridge and the humeral head lies a lateral tuberosity that is oval with a proximomedially–distolaterally orientated long axis. Centrally on the lateral surface of the proximal humeral extremity a proximodistally oval, caudolateral rugosity is developed. The humerus of *Congosaurus bequaerti* (Text-fig. 9F) and *Hyposaurus* (YPM 764) bears laterodistal to the caudolateral rugosity a sulcus orientated in the long axis of the humerus. The lateral condyle of the distal extremity of the humerus is one-fifth larger than the medial condyle, but the latter projects more distally (Text-fig. 9G). Both condyles are separated by a deep intercondylar sulcus. The medial and lateral epicondyles of the humerus of the Hyposaurinae form weak rugosities.

Ulna and radius. A right ulna (MRAC 1818), which is broken into two pieces, and a proximal fragment of a radius (MRAC 1820) are known for *Congosaurus bequaerti* (Jouve and Schwarz 2004). The ulna of *Congosaurus* was erroneously described as a tibia by Swinton (1950). From *Hyposaurus rogersii*, a left ulna and radius (YPM 8145) are preserved (Parris 1986). The ulna reaches three-quarters of the length of the humerus. The shaft of the ulna has a longitudinally oval cross-section and a concave cranial and slightly convex caudal margin (Text-fig. 9I).

The head of the ulna is slightly bent craniomedially and twice as wide as the distal extremity of the ulna. In its medial half the articular surface of the ulnar head bears a circular condylar pit and, lateral to the fovea, a central circular tuber. The centrally depressed articular surface with the radius is rounded rectangular and is bevelled cranioventrally from the cranial margin of the ulnar head (Jouve and Schwarz 2004). Around the articular surface with the radius, the craniolateral surface of the proximal ulnar extremity is rugose. The olecranon forms a prominent and strongly rugose, proximodistally oval tuberosity that covers the caudal surface of the proximal extremity of the ulna (Text-fig. 9I). At the transition between the proximal extremity and the shaft of the ulna, a proximodistally oval rugosity with a central nutricious foramen is developed.

In contrast to that of *Crocodylus porosus*, the ulna of the Hyposaurinae possesses a cranial hemicondyle at its distal extremity that is separated from the caudal hemicondyle by a central indentation (Text-fig. 9I; Langston 1995). The lateral surface of the lateral hemicondyle and the medial surface of the medial hemicondyle are covered with proximodistally orientated striae. At the transition from the distal extremity to the ulnar shaft the lateral ulnar surface bears a proximodistally oval, slightly rugose depression.

The radius reaches two-thirds of the length of the ulna. The radial shaft is lateromedially oval in cross-section and reaches two-thirds of the width of the head of the radius. The width of the radial head is four-fifths of the width of the ulnar head (Jouve and Schwarz 2004). In proximal view, the radial head is lateromedially kidney-shaped with a convex cranial margin and a concave caudal margin, and shows a central depression. The ulnar articular surface is bevelled from the caudal margin of the radial head and forms a rounded rectangular area with a weak, circular lateral and medial tuber. Distally adjacent to the ulnar articular surface the caudal surface of the proximal radial extremity is rugose.

The lateral surface of the radial shaft bears a proximodistally orientated crest medially. On the medial surface of the radial shaft, on the transition to the distal radial condyle, there is a proximodistally orientated, rugose crest. The distal radial condyle is rounded rectangular in outline. The distal articular surface of the radius is surrounded by striae that are most expressed on the lateral and medial surface of the distal radial extremity.

Radiale. The right radiale of *Congosaurus bequaerti* (MRAC 1819; Jouve and Schwarz 2004) reaches one-quarter of the length of the ulna. The body of the radiale is constricted and comprises one-quarter of the total length of the radiale (Text-fig. 9J–K). In proximal view, the articular surfaces with radius and ulna form one single kidney-shaped, centrally depressed radioulnar articular surface. From this surface, the articular surface for the ulnare curves to the medial margin of the radiale and extends distally to the proximal third of the length of the radiale (Text-fig. 9K). The articular surface for the ulnare is rounded-quadrangular in outline and distally ends in a craniolateral rugosity. A caudal tuberosity protrudes from the caudal surface of the radiale (Text-fig. 9J–K). At the distal extremity of the radiale, the metacarpal articular surface is rounded-triangular in outline and surrounded by a striated rim.

Metacarpals. In the partial skeleton of *Congosaurus bequaerti*, four metacarpals are preserved, which reach one-sixth of the humerus length (Jouve and Schwarz 2004). Three isolated metacarpals are also present in *Hyposaurus* sp. (YPM 8148). The metacarpals have a constricted shaft and a spatulate basis with a convex proximal articular surface. In one metacarpal of *Congosaurus* (MRAC 1825) and *Hyposaurus* sp. (YPM 8148) the base is twisted laterally at an angle of 90 degrees to the shaft (Text-fig. 9L–M). Distal to the proximal articular surface the base of the metacarpal is laterally and medially rugose and on its dorsal surface bears a median circular tuberosity. The distal articular surface for the carpus is divi-

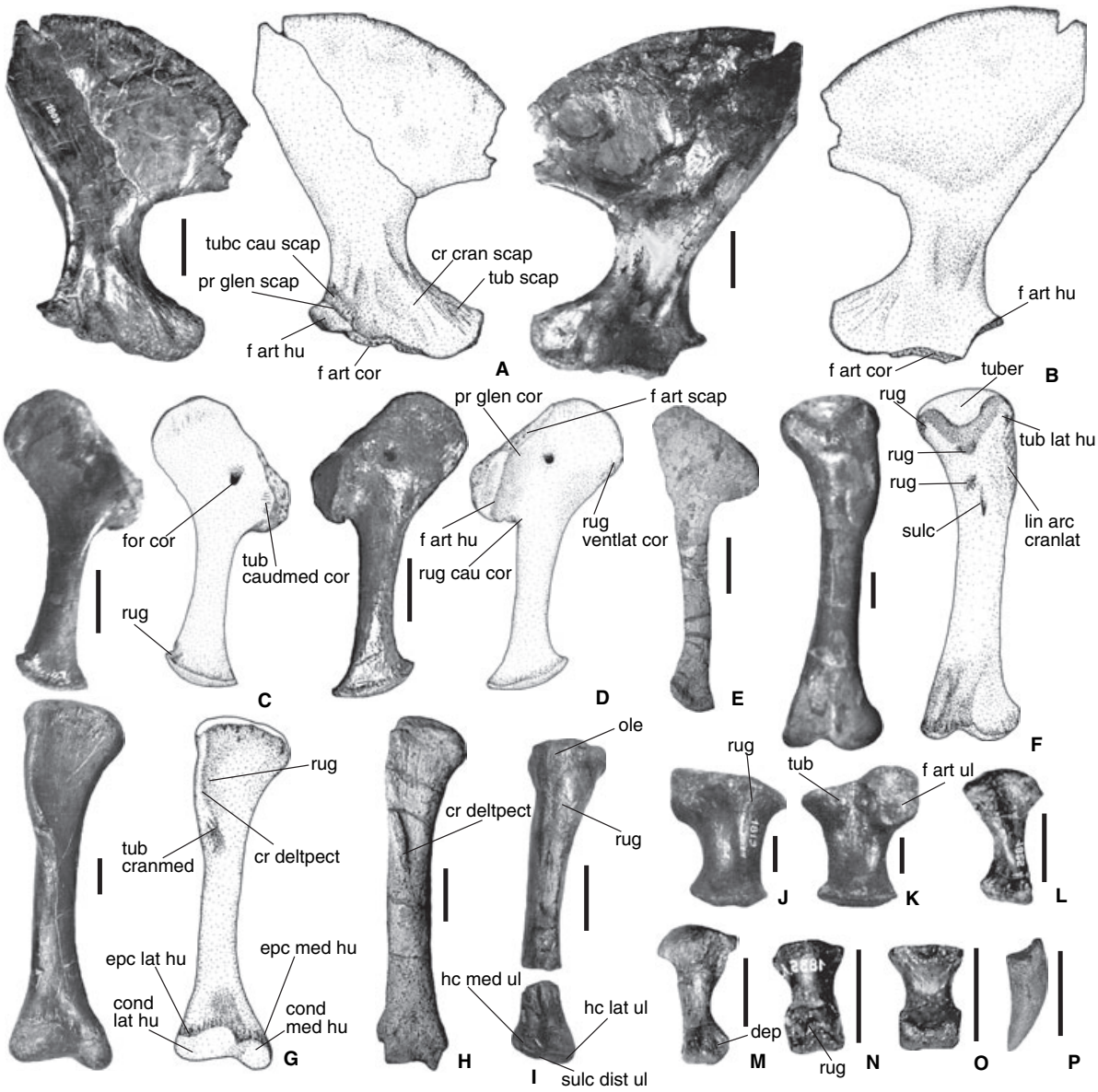

TEXT-FIG. 9. Photographs and drawings of elements of the pectoral girdle and forelimbs of the Hyposaurinae. A–B, photographs (left) and drawings (right) of right scapula (MRAC 1809) of *Congosaurus bequaerti*. A, lateral view; B, medial view. C–D, photographs (left) and drawings (right) of right coracoid (MRAC 1811) of *Congosaurus bequaerti*. C, medial view; D, lateral view. E, photograph of right coracoid of *Hyposaurus derbianus* (BMNH 315), medial view. F–G, photographs (left) and drawings (right) of right humerus (MRAC 1813) of *Congosaurus bequaerti*. F, lateral view; G, medial view. H, photograph of right humerus of *Hyposaurus derbianus* (BMNH 315), medial view; the lateral and medial part of the distal extremity is broken away. I, photograph of right ulna of *Congosaurus bequaerti* (MRAC 1818), caudal view. J–K, photographs of radiale of *Congosaurus bequaerti* (MRAC 1819). J, dorsal view; K, ventral view. L–M, photographs of metapodium of *Congosaurus bequaerti* (MRAC 1826). L, dorsal view; M, plantar view. N–O, photographs of phalanx of *Congosaurus bequaerti* (MRAC 1835 A). N, dorsal view; O, plantar view. P, photograph of ungual phalanx of *Congosaurus bequaerti* (MRAC 1828), lateral view. Scale bars represent 50 mm in A–I and 20 mm in J–P.

ded into a medial and a lateral condyle by a median indentation. The dorsal surface of the carpal articular surface is medially depressed and rugose. The lateral margins of the proximal metacarpal extremity are broadened and bear a median circular depression (Text-fig. 9L–M).

Ilium. In the Hyposaurinae, the dorsal half of the ilium is formed by the iliac wing, which is slightly convex caudal to the craniodorsal tubercle in *Congosaurus* (Text-fig. 10A–B; Jouve and Schwarz 2004), cf. *Rhabdognathus* (Langston 1995), and cf. *Hyposaurus* (Storrs 1986). In *Hyposaurus natator* (YPM 753,

Troxell 1925, fig. 13) the dorsal margin of the iliac wing is concave immediately caudal to the craniodorsal tubercle and convex only in its caudal half. The dorsal margin of the iliac wing is covered by prominent, lateromedially orientated striae (Text-fig. 10A). The caudal margin of the ilium forms a semicircular postacetabular recess (Text-fig. 10B; Troxell 1925). The craniov-entrally directed acetabular peduncle and the ventrally directed ischiac articular surface descend from the ventral margin of the ilium, separated from each other by a semicircular acetabular concavity. The craniodorsal tubercle of the iliac wing has a weakly convex and rugose dorsal margin and, in contrast to *Crocodylus porosus*, is positioned dorsal to the first sacral rib (Text-fig. 10A–B).

The lateral surface of the iliac wing bears a caudolateral tuberosity in its caudodorsal part, followed by a caudal tuberosity in the caudodorsal corner of the ilium (Text-fig. 10A). The bowl-shaped acetabular fossa extends for the medial two-thirds of the lateral surface of the ilium. The acetabular fossa on the ilium of the Hyposaurinae is more deeply concave than that of *Crocodylus porosus*. A prominent, dorsally convex supra-acetabular crest separates the acetabular fossa from the iliac wing (Text-fig. 10A). The acetabular tuberosity sits in the dorsal half of the fossa. In medial view, the sacral symphysial surfaces extend to the ventral half of the medial surface of the ilium (Text-fig. 10B). They are separated from each other by a median bulge.

Ischium. The ischium is twice as high as the ilium medially. Its shaft is weakly constricted. Based on a single broken ischium, Troxell (1925) described the ventral ischiac wing of *Hyposaurus natator* (YPM 753) as narrow and rod-like (DS, pers. obs. 2004). However, other more complete finds of dyrosaur ischia (i.e. Text-fig. 10C–D; Storrs 1986; Langston 1995) show that the ischiac wing of the Hyposaurinae is spatulate and ends with a weakly convex ventral margin.

The caudal ischiac process and the subacetabular process are separated from each other by a semicircular ischiac acetabular concavity (Text-fig. 10C–D). The acetabular foramen is longitudinally oval in outline and bordered in its ventral two-thirds by the ischium (Troxell 1925; Storrs 1986; Langston 1995). The caudal ischiac process is twice as long as the subacetabular process and ends dorsally with a rugose iliac articular surface. A ventrally facing pubic articular surface occupies the ventral two-thirds of the cranial surface of the subacetabular process. This process bears a dorsally directed iliac articular surface in its dorsal third and a medial rugosity on its medial surface (Text-fig. 10C). From the base of the subacetabular process, a craniolateral depression continues over the cranial margin of the ischium ventrally (Text-fig. 10C).

The lateral surface of the ischiac shaft bears an arched ischiac ridge that runs from the ventral margin of the subacetabular process to the ventral margin of the ischium (Text-fig. 10D). The lateral and medial surfaces of the ischiac wing are covered by delicate, proximodistally orientated striae.

Pubis. The pubis is one-quarter longer than the ischium and reaches three-quarters of the length of the femur. The pubic shaft has a nearly circular cross-section. The coxal extremity of the pubis is one-third wider than the pubic shaft. The spatulate pubic wing forms the cranial half of the pubis and has a strongly concave dorsal margin. The dorsal part of the ventral margin of the pubic wing is weakly concave and blade-like (Text-fig. 10E). The pubis ends cranially with a faintly convex and broadened, bulge-like margin, from which a strong rugosity continues to the lateral and medial surface of the pubic wing. In *Hyposaurus natator* (YPM 753), the ventral margin of the wing of the left pubis possesses a median sulcus in which the ventral margin of the wing of the right pubis inserts, so that both pubic bones are connected. These medially fused bones were figured and described by Troxell (1925), but interpreted to be the result of diagenesis by Langston (1995). However, following an examination of the material by one of us (DS) in 2004, the connection between left and right pubic bone in *Hyposaurus natator* is interpreted to be natural, as decribed by Troxell (1925). Since the pubic bones of *Hyposaurus natator* (YPM 753) are so far the only complete ossa pubes known from the Hyposaurinae, the possibility of a connection between left and right ventral pubic margin in other Hyposaurinae cannot be excluded.

The articular surface of the coxal extremity of the pubis is longitudinally oval and surrounded by striae. The lateral surface of the pubic wing of *Dyrosaurus* sp. (SMNK-PAL 3826 72/94) bears a dorsoventrally oval depression at its cranial margin (Text-fig. 10E).

Femur. The femur is sigmoidally curved. Its shaft is straight and has a longitudinally oval cross-section. The proximal and distal extremities are twisted at an angle of 140 degrees against each other and are one-quarter wider than the femoral shaft.

The proximal extremity of the femur curves cranially at an angle of 45 degrees to the long axis of the femur (Text-fig. 10F–G). The femoral head is asymmetrically oval in outline. A median bar descends from the femoral head across the lateral surface of the proximal extremity (Text-fig. 10F). The smooth surface of the head is separated from the rugose medial and lateral surface of the proximal femoral extremity by a rounded step.

The caudal surface of the proximal extremity of the femur bears a caudal rugosity that continues laterally into a caudolateral tuberosity (Text-fig. 10F). The lateral surface of the proximal extremity is slightly concave and bears a proximodistally oval proximal depression cranial to the caudolateral tuberosity. Distally adjacent to the proximal depression there is a weakly rugose, proximodistal oval depression (Text-fig. 10F).

The femoral ('fourth') trochanter is a prominent bulge at the transition from the medial surface of the proximal extremity to the caudal surface of the femoral shaft and distocaudally ends with a rugosity (Text-fig. 10G). The femoral trochanter is cranially bordered by a shallow, proximodistally oval paratrochanteric fossa. Distal to this fossa is a small, circular depression, caudodistal to which a rugose, craniocaudally oval, medial depression is developed (Text-fig. 10G). A caudal depression is present on the caudal surface of the femoral shaft distal to the femoral trochanter.

The distal extremity of the femur is divided into lateral and medial condyles, which are separated from each other by an intercondylar fossa (Text-fig. 10G). The medial condyle is one-sixth longer, but one-quarter narrower than the lateral condyle.

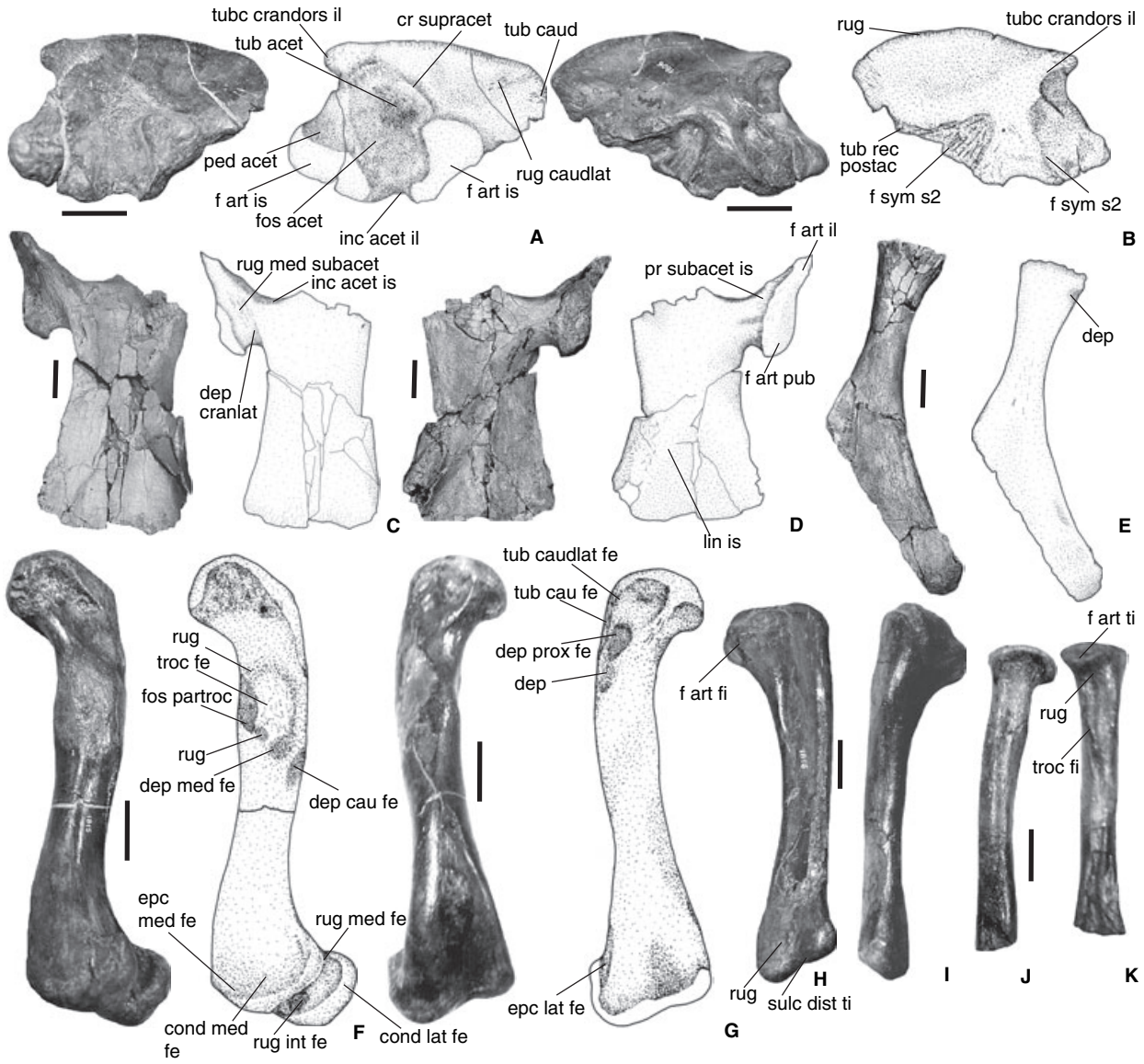

TEXT-FIG. 10. Photographs and drawings of elements of the pelvic girdle and hindlimbs of the Hyposaurinae. A–B, photographs (left) and drawings (right) of left ilium of *Congosaurus bequaerti* (MRAC 1806). A, lateral view; B, medial view. C–D, photographs (left) and drawings (right) of right ischium (SMNK 3826 73/94) of *Dyrosaurus* sp. C, medial view; D, lateral view. E, photograph (left) and drawing (right) of right pubis (SMNK-PAL 3826 72/94, caudal part of ala pubica is missing) of *Dyrosaurus* sp., lateral view. F–K, elements of the hindlimbs of *Congosaurus bequaerti* (MRAC). F–G, photographs (left) and drawings (right) of right femur (MRAC 1815). F, craniomedial view; G, caudolateral view. H–I, right tibia (MRAC 1816). H, cranial view; I, caudal view. J–K, left fibula (MRAC 1814). J, cranial view; K, caudal view. For abbreviations, see text. Scale bars represent 50 mm.

At the caudal surface of the distal extremity each condyle forms a bulge that continues proximally up to the transition between the distal extremity and the shaft of the femur and bears a rugosity on its medial surface (Text-fig. 10G). Between the lateral and medial condylar bulge on the caudal surface of the distal extremity, there is a median intermediate rugosity inside the intercondylar fossa (Text-fig. 10G). The lateral and medial condyles form a lateral and medial epicondyle, respectively, on the cranial surface of the distal femoral extremity. Proximal to the lateral epicondyle is a distolateral tubercle.

Tibia and fibula. The tibiae of *Congosaurus* (MRAC 1817; Jouve and Schwarz 2004), *Hyposaurus* sp. (YPM 8146) and *Dyrosaurus* '*paucidens*' (Arambourg 1952) reach 75 per cent of the length of the femur; the tibia of cf. *Rhabdognathus* (Langston 1995) reaches 85 per cent. The tibia of the Hyposaurinae has a straight shaft, from which the proximal extremity curves laterally at 30 degrees (Text-fig. 10H–I). The proximal extremity is twice as wide as the distal extremity, which is one-fifth wider than the shaft. The medial margin of the shaft is strongly concave and the lateral margin slightly concave.

The articular surface of the tibial head is irregularly rounded in outline and bears a central condylar pit. The articular surface with the fibula descends from the cranial margin of the tibial head over the cranial surface of the proximal extremity and ends distally with a lateral tuberosity (Text-fig. 10H–I). At the transition between the proximal extremity and the shaft medially is a large, proximodistally oval, proximal craniomedial tuberosity. The distal craniomedial tuberosity is positioned in the distal quarter of the tibial shaft. At the distal extremity of the tibia, the articular surface with the astragalus is divided by a median sulcus into a medial and a lateral half (Text-fig. 10H; Langston 1995). The medial part of the articular surface with the astragalus forms a rounded distal projection and bears a distal craniomedial rugosity on its cranial surface.

Fibular fragments of cf. *Rhabdognathus* were described by Langston (1995), and a proximal fragment of a left fibula is known from *Congosaurus* (MRAC 1811; Jouve and Schwarz 2004). Arambourg (1952, pl. 44, fig. 8) described and figured as a fibula a long bone of *Dyrosaurus* '*paucidens*' that might be a metatarsal bone.

The fibula of cf. *Rhabdognathus* and *Congosaurus* possesses a fibular head with a convex articular surface. Caudomedially on the head a circular condylar pit is developed. The fibular head forms a craniolateral articular surface for the tibia that is bevelled to the craniolateral surface of the proximal extremity of the fibula, where it is followed by a rugosity (Text-fig. 10J–K).

The cross-section of the fibular body is lateromedially oval. In *Congosaurus*, the fibular trochanter forms a smooth craniolateral crest that runs from the proximal extremity across the proximal fifth of the length of the fibular shaft distally (Text-fig. 10J). Distally, the astragalar part of the proximotarsal articular surface of the fibula of cf. *Rhabdognathus* curves to the lateral surface of the distal extremity whereas its calcanear part forms a rounded, distally directed, projection (Langston 1995).

Tarsals. We here refer to the detailed description of the morphology of the astragalus and calcaneum of cf. *Rhagdognathus* by Langston (1995). An astragalus and calcaneum of *Hyposaurus* sp. (AMNH no. 2389), and the astragalus of an undetermined dyrosaurid crocodilian from Mali (MNHN IF indet.) are similar to the bones described by Langston (1995). The description of an astragalus of cf. *Hyposaurus* by Storrs (1986) is too superficial to provide anatomical details. According to these descriptions, the main differences between the astragalus of the Hyposaurinae and the extant crocodilians are a wider saddle-shaped tibial articular surface and a stout calcaneal articular process that extends deeper into the astragalar cotyle of the calcaneum than in *Crocodylus* and *Alligator* (Langston 1995). The calcaneum of the Hyposaurinae bears a calcaneal tuber, which is approximately one-third broader and shorter than that of *Crocodylus* and *Alligator* (Langston 1995).

Metatarsals. Cf. *Rhabdognathus* possesses five metatarsals (Langston 1995). The first–fourth metatarsals are preserved in the partial skeleton of *Congosaurus* (Jouve and Schwarz 2004) and an isolated metatarsal is known from *Hyposaurus* sp. (YPM 8147). The first–fourth metatarsals reach at least one-third of the length of the femur and, with the exception of a relatively longer shaft, are similar to the metacarpals (see above). The fifth metatarsal of cf. *Rhabdognathus* possesses a broad, flat articular surface for the quarter metatarsal, whereas in *Crocodylus* and *Alligator* the articular surface for the fourth metatarsal bone of the fifth metatarsal bone forms a short tuber (Langston 1995).

Phalanges. The total number of phalanges of manus and pes is not known for the Hyposaurinae. The phalanges of *Congosaurus* (Jouve and Schwarz 2004), *Hyposaurus* sp. (YPM 8148) and cf. *Rhabdognathus* (Langston 1995) possess a constricted body (Text-fig. 9N–O). In proximal view the proximal base of the phalanx ends with a kidney-shaped, concave articular surface. The distal extremity possesses broadened lateral and medial surfaces with a median circular depression. The distal tarsal articular surface is medially indented. The dorsal surface of the base and the distal extremity of the phalanges is centrally rugose (Text-fig. 9N–O). The preserved ungual phalanges of *Congosaurus* are strongly dorsally curved and taper distally to a pin-like process (Text-fig. 9P).

Osteoderms

Nuchal osteoderms. An osteoderm of cf. *Rhabdognathus* possibly belonging to a neck shield was figured by Langston (1995). It remains uncertain whether or not a nuchal shield existed in the Hyposaurinae. If so, there is no way to reconstruct its configuration on the basis of available evidence.

Dorsal osteoderms. Isolated dorsal osteoderms are known from *Dyrosaurus* spp. (SMNK-PAL 3826, MNHN Coll. Arambourg; MNHN Coll. Lavocat), *Hyposaurus* (BMNH no. 315, YPM 380, YPM 323, 17827; Denton *et al.* 1997), *Congosaurus bequaerti* (MRAC; Jouve and Schwarz 2004), cf. *Rhabdognathus* (Langston 1995), cf. *Sokotosaurus* (MNHN 1964-27 663) and from indetermined Dyrosauridae (e.g. BMNH R. 5635; 11056, MNHN Coll. Arambourg; Coll. Lavocat; Coll. Swinton). In contrast to recent Crocodilia, the dorsal osteoderms possess no external keel, which is mirrored in their description as 'biscuit-like' (Swinton 1950) or 'soda-cracker-like' (Langston 1995). The external surface of the osteoderms bears a pattern of concentrically distributed deep oval pits (Text-fig. 11). The internal surface of the osteoderms is crossed by a few, randomly distributed grooves and is perforated by 2–3 nutricious foramina (Text-fig. 11).

The paravertebral osteoderms are rectangular in outline and between 1·1 times and twice as wide as long. Their external surface is slightly vaulted (Text-fig. 11E–F), and their lateral margin from the medial and caudal region of the trunk bears a triangular craniolateral process (Text-fig. 11C–D), whereas in the paravertebral osteoderms from the cranial region of the trunk there is a short, laterally convex craniolateral projection (Text-fig. 11A). In dorsal view, parallel to the lateral margin, the external surface is lowered and separated from the rest of the external surface by a sharp, medially convex margin. This margin is most strongly concave in the paravertebral osteoderms from the caudal region of the trunk (Text-fig. 11C–D). The cranial tenth of the external surface of the paravertebral osteoderms is smooth and forms an articular surface (Text-fig. 11A–C). The medial margin of these osteoderms is serrated and slightly bevelled, with a few lateromedially orientated striae (Text-fig. 11B, F).

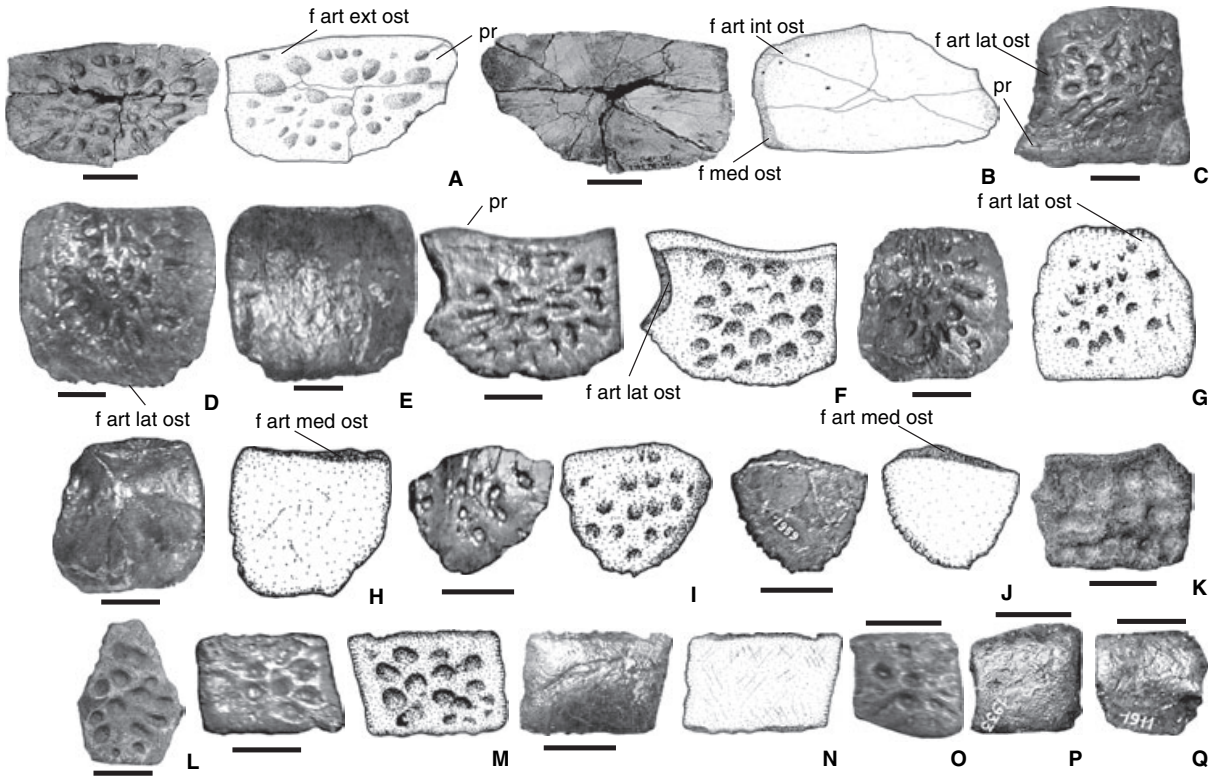

TEXT-FIG. 11. Photographs and drawings of osteoderms of the Hyposaurinae. A–B, photographs (left) and drawings (right) of paravertebral osteoderm of *Dyrosaurus* sp. (SMNK-PAL 85/94). A, external view; B, internal view. C–J, dorsal osteoderms of *Congosaurus bequaerti* (MRAC). C, photograph of paravertebral osteoderm (MRAC 1954), external view. D–E, photograph of paravertebral osteoderm (MRAC 1944). D, external view; E, internal view. F, photograph (left) and drawing (right) of paravertebral osteoderm (MRAC 1960). G–H, photographs (left) and drawings (right) of accessory osteoderm (MRAC 1968). G, external view; H, internal view. I–J, photographs (left) and drawings (right) of accessory osteoderm (MRAC 1959). I, external view; J, internal view. K, gastral osteoderm (BMNH R.5635) of an undetermined dyrosaurid, external view. L, gastral osteoderm (BMNH R.5642) of an undetermined dyrosaurid, external view. M–Q, gastral osteoderms of *Congosaurus bequaerti* (MRAC). M–N, photographs (left) and drawings (right) of gastral osteoderm (MRAC 1906). M, external view; N, internal view. O–P, gastral osteoderm (MRAC 1933). O, external view; P, internal view. Q, gastral osteoderm (MRAC 1911), internal view. For abbreviations, see text. Scale bars represent 20 mm.

The accessory osteoderms of the medial region of the trunk are square in outline (Text-fig. 11G–H), whereas those of the cranial and caudal region of the trunk are rounded-triangular (Text-fig. 11I–J). The accessory osteoderms are up to one-third smaller than the paravertebral osteoderms. The medial margin of the accessory osteoderms is straight. Parallel to the medial margin, the internal surface is lowered and ends with a laterally convex margin (Text-fig. 8H, J). As in the paravertebral osteoderms, the concavity is deepest in the accessory osteoderms from the caudal region of the trunk. In the dorsal shield, the medial margin of the accessory osteoderms medially overlaps the lateral margin of the paravertebral osteoderm, forming a squamose suture. This suture is lateromedially narrowest in the medial transverse rows of the trunk.

In the partial skeleton of *Congosaurus*, an accessory osteoderm with a strongly serrated lateral margin (MRAC 1945) indicates that in the medial region of the trunk the transverse rows consisted of at least two accessory osteoderms on both sides (Text-fig. 12; see below).

Configuration of the dorsal armour. The great number of disarticulated dorsal osteoderms of the partial skeleton of *Congosaurus bequaerti* (MRAC) makes a detailed reconstruction of its dorsal osteodermal shield possible (Text-fig. 12). The similarity between the isolated dorsal osteoderms of different hyposaurine taxa indicates that their dorsal armour resembled that of *Congosaurus*.

The dorsal osteodermal shield comprises two longitudinal rows of paravertebral osteoderms (Text-fig. 12) and two lateral rows of acccessory osteoderms, forming at least 12 transverse rows. In the medial region of the trunk, the transverse rows comprise one paravertebral and at least two accessory osteoderms.

A comparison between the width of the transverse processes and the width of the paravertebral osteoderms of *Congosaurus* indicates the positions of the osteoderms within the trunk, as seen in teleosaurid thalattosuchians (Westphal 1962; Frey 1988*b*; Vignaud 1995). The width of the paravertebral osteoderms increases from cranial to caudal and reaches a maximum

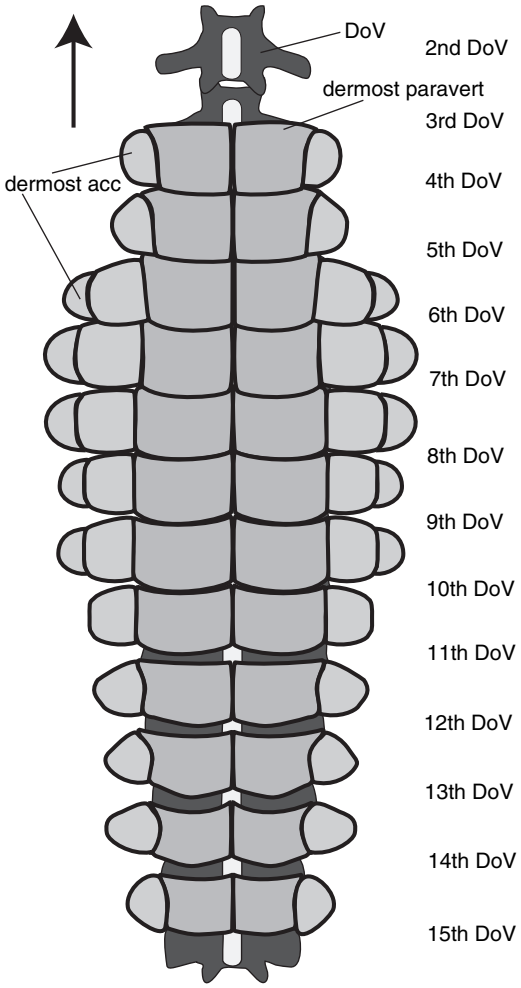

TEXT-FIG. 12. Reconstruction of the dorsal osteodermal shield of *Congosaurus bequaerti* in dorsal view based on isolated dermostea from the partial skeleton in the MRAC. Arrow indicates cranial direction. For abbreviations, see text.

between the sixth and the tenth dorsal vertebrae. Caudal to the tenth dorsal vertebra the width of the paravertebral osteoderms decreases again. The cranialmost osteoderm slightly overlaps the caudally following paravertebral osteoderm. The third–fifth paravertebral osteoderms imbricate. Caudal to the fifth paravertebral osteoderm their length decreases to less than the length of a vertebral body.

Ventral osteodermal shield and ventral osteoderms. Isolated ventral osteoderms are rectangular in outline and possess serrated lateral and smooth, bevelled, cranial and caudal margins (Text-fig. 11M–N). They are preserved in *Congosaurus* (e.g. MRAC 1906, 1911, 1933), *Hyposaurus* (BMNH 315), cf. *Rhabdognathus* and an undetermined dyrosaurid (BMNH 5642). Gastral osteoderms with a pentagonal and hexagonal outline and strongly serrated margins (Text-fig. 11K–L) are reported in *Congosaurus* (MRAC 1910), cf. *Rhabdognathus* (Langston 1995) and an undetermined dyrosaurid (BMNH R.5635, R.5636, R.5642; Salisbury 2001). Rectangular osteoderms from a marginal position in the gastral osteodermal shield are known from *Congosaurus* (Text-fig. 11O–Q).

The external surface of the ventral osteoderms is covered with a few, concentrically orientated oval pits. The internal surface of the ventral osteoderms is covered by a mesh of delicate striae crossing each other at acute angles of about 70 degrees (Text-fig. 11N).

The gastral armour of the Hyposaurinae presumably consists of one part with imbricating transverse rows of rectangular osteoderms and another with hexagonal, suturally connected osteoderms. These two parts are connected by at least one row of pentagonal ventral osteoderms. Due to the lack of an articulated ventral osteodermal shield, neither the extent nor the position of the two parts can be reconstructed. It is possible that, corresponding to the configuration of the ventral armour with similar ventral osteoderms in *Pholidosaurus* (Salisbury 2001), in the ventral armour of the Hyposaurinae the cranial part comprised transverse rows of rectangular osteoderms whereas the caudal part consisted of hexagonal osteoderms.

Other osteoderms. The partial skeleton of *Congosaurus* also comprises some small, asterisk-shaped osteoderms, probably from the region of the limbs.

DISCUSSION

Skeletal reconstruction

The investigation of the new hyposaurid material confirms the reconstruction provided by Langston (1995) with respect to the morphology of the neural spines and the haemal arches. However, the heights of the neural spines of the neck and the midpart of the trunk were underestimated. The shape of the scapula, as reconstructed by Langston (1995), must be corrected by the new finds: its caudal margin is concave and its dorsal margin is strongly convex, as evidenced by *Congosaurus* (Swinton 1950; Jouve and Schwarz 2004), *Hyposaurus* (YPM 764) and *Dyrosaurus* (S. Jouve, pers. comm. 2002). The assumption of Hua (1997) that the neural spines are of approximately equal height from the third cervical to the third caudal vertebra (Text-fig. 1B) must be rejected according to the data presented here. The scapula depicted in Hua's (1997) reconstruction (Text-fig. 1B) is much too small and lacks the expanded dorsal blade visible in the scapulae of *Congosaurus* and *Dyrosaurus* (Text-fig. 9A–B). Hua (1997) furthermore wrongly reconstructed the girdles of the Hyposaurinae as small and similar to those of other crocodilians.

An unresolved discrepancy in the reconstructions of hyposaurine postcrania concerns the position of the first haemal arch. In *Congosaurus*, this arch is articulated between the third and fourth caudal vertebrae, whereas in other hyposaurine dyrosaurs it appears to articulate between the second and third caudal vertebrae, as in

other crocodilians (Frey 1988*a*). There are three possible explanations to this phenomenon:

1. The *Congosaurus* skeleton represents a pathological specimen with respect to the lack of the first haemal arch. This possibility can only be confirmed by further fossil evidence.

2. The position of the first haemal arch in *Congosaurus* is diagnostic for the genus or the species. This possibility can also only be confirmed by further fossil evidence.

3. The different positions of the first haemal arches within the Hyposaurinae correspond to sexual dimorphism, in which the females lack a haemal arch between the second and the third caudal vertebrae in order to increase the diameter of the egg passage. In recent crocodilians, the first haemal arch articulates between the second and the third caudal vertebrae. In females, it is shorter and more slender than those that follow it and the cranial margin is oblique (Frey 1988*a*; EF and DS, pers. obs. 2004). As a consequence, the terminal part of the cloaca would have had a larger diameter than in males, which could have been advantageous for egg-laying. In males, the first haemal arch is the longest of the sequence and sometimes twice as wide as the second (e.g. in *Piscogavialis jugaliperforatus* Kraus 1998, SMNK-PAL 1282). It is likely that the retractor muscles of the penis were partly inserted on this haemal arch. If we assume that the lack of the first haemal arch in *Congosaurus* is a result of sexual dimorphism, the specimen described by Swinton (1950) and Jouve and Schwarz (2004) could indicate a female individual. Again, this hypothesis can only be confirmed by further fossil evidence.

Implications for biomechanics of the axial skeleton and reconstructable locomotor modes

The differences between the postcranial osteology of hyposaurine dyrosaurs and that of all other crocodilians does have consequences for the reconstruction of the soft-part elements, especially for the bracing system. It has been demonstrated that the dorsal osteodermal shield, together with the equally high neural spines and the horizontally orientated transverse processes, acts as a segmented I-beam carrier, which is braced and moved by the hydraulic epaxial muscle masses (Frey 1988*b*; Salisbury 2001; Salisbury and Frey 2001). This system can only work if the angle of attack in the epaxial muscle to the bony elements of the system is about 5 degrees (Gans and Bock 1965; Gans and DeVree 1987; Frey 1988*b*; Tarsitano *et al.* 1988; Salisbury 2001).

For the hyposaurine dyrosaurs we can postulate that a classical crocodilian bracing system cannot work. If the low angle of muscular attachment is 5 degrees to the osteoderms, the lengths of the muscle segments would become physiologically impossible. We therefore assume that the epaxial muscle segments were the same lengths as in extant crocodilians, so that the angle of attachment to the osteoderms would be about 20 degrees. With this reconstruction, m. transversospinalis forms a cross-girder structure along the lateral surfaces of the neural spines (Text-fig. 13), whereas the myoseptal cones of m. tendinoarticularis and m. longissimus dorsi are dorsoventrally expanded and medially open, so that their muscle fibres could unite to form central fascicles (Text-fig. 13). Such a configuration of the epaxial musculature would apply less longitudinal bending loads to the paravertebral osteoderms of the Hyposaurinae than in recent crocodilians and may be why external osteodermal keels are missing in Hyposaurinae. Furthermore, in hyposaurine dyrosaurs, the high neural spines with respect to the vertebral bodies as well as the lateral extension of the transverse processes have consequences for the dimensions of the epaxial muscles.

Due to the large oval diameter of the medial epaxial muscles and their insertion on the lateral surfaces of the

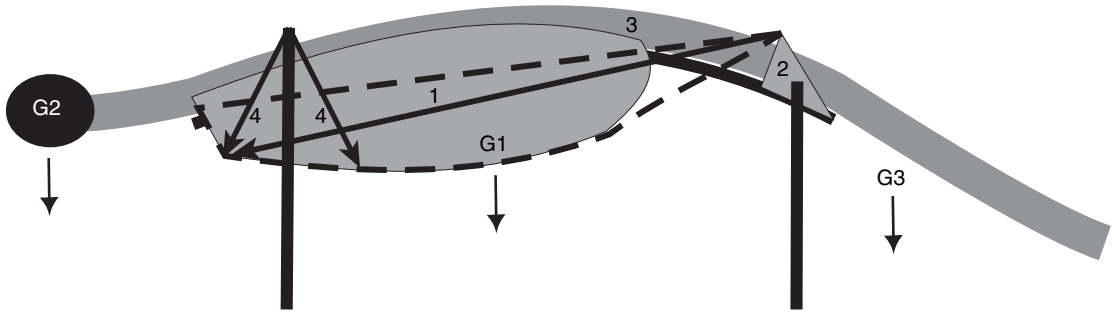

TEXT-FIG. 13. Aspects of bracing of the trunk in the Hyposaurinae. M. iliocostalis (1, outline of insertion is indicated by hatched lines) inserted at a steeper angle to the horizontal plane at the ilium (2) than in recent crocodilians and most probably participated in the bracing of the trunk. The bracing of the trunk is reconstructed to resemble a segmented, hydraulically stabilised string-and-arch construction in which the arch is formed by the chain of vertebral segments with epaxial musculature (3) and the string is formed by the m. iliocostalis system. The thorax and the cervical vertebral column are suspended from the scapula by means of the m. serratus system (4). The trunk, neck and tail are loaded by gravity G1–G3.

neural spines (Schwarz 2003; Schwarz *et al.* in prep.) the forces of the epaxial musculature in the Hyposaurinae must have acted directly on the neural spines and from there were transmitted on the vertebrae, without invoking a force transmission system via the paravertebral osteoderms as in recent crocodilians (Frey 1988*b*; Salisbury 2001).

In the tail of the Hyposaurinae, the increase in height of the neural spines resulted most likely in an increase in the diameter of the cross-section of the epaxial musculature. From the reconstructed dimensions of the expaxial tail base muscles it appears also likely that here the tendons of m. transversospinalis as well as the myosepts of m. tendinoarticularis and longissimus caudae were longer than in the trunk. If so, large longitudinal bending loads acted on the dermis of the tail. These bending loads could have been compensated for by external keels at the scutes of the tail skin.

The high craniodorsal tubercle of the ilium of the Hyposaurinae indicates that m. iliocostalis of hyposaurine dyrosaurs inserted at a steeper angle to the horizontal plane (Text-fig. 13) than in recent crocodilians (Frey 1988*a*, *b*; Salisbury 2001). The long and vertically orientated laterocostal segments of the thoracic ribs of the Hyposaurinae provide evidence for a vertically orientated m. iliocostalis with a large oval cross-section, which most probably participated in the bracing of the trunk.

According to the reconstructions briefly outlined above, the bracing of the trunk of the hyposaurine dyrosaurs technically resembles a segmented, hydraulically stabilised string-and-arch construction (Text-fig. 13). The arch is formed by the chain of vertebral segments, each representing an inverse T-beam. The string is formed by the m. iliocostalis system. The dorsal osteodermal armour allowed considerable ventral and lateral flexibility of the caudal trunk region, but strongly limited dorsal flexibility of the trunk.

The bracing system of the hyposaurine trunk postulated above does not allow for stabilisation of the vertebral column against the combination of mechanical loads. The Hyposaurinae possessed amphicoelous vertebrae, which could not counteract dorsoventral shear loads. The angles of the articular surfaces of the zygapophyses of the dorsal vertebrae were about 50 degrees to the vertical median plane and therefore were less able to counteract dorsoventral shear loads than in the recent crocodilians, and certainly could not adequately counteract transverse shear loads. Additionally, the lateral musculature of the body wall was positioned ventral to the vertebral column and could not contribute to the stabilisation of the vertebral column against transverse shear loads. Therefore, the overall construction of the hyposaurine trunk probably did not accommodate the combination of mechanical loads, in particular dorsoventral and transverse shear loads.

As a consequence of this reduced capability to accommodate the combination of mechanical loads, terrestrial locomotor modes such as high-walk and gallop in the Hyposaurinae were most probably restricted to individuals with less than 50 kg of mass (2·3 m total length), similar to *Gavialis gangeticus* (Bustard and Singh 1977; Salisbury 2001). In contrast, as also indicated by the enormous tail musculature, aquatic locomotion by axial and hybrid swimming can be regarded in the Hyposaurinae has having greater velocity and stamina than in the recent crocodilians. These reconstructions are in accordance with the distribution and kind of localities yielding remains of hyposaurine dyrosaurids, comprising mostly marine and epicontinental, but to a lesser extent also estuarine and fluviatile deposits.

A detailed reconstruction of the bracing system of hyposaurine dyrosaurs is beyond the scope of this paper and will be presented elsewhere. Discussion of the bracing system will allow a detailed survey of the locomotor options of these animals, but also requires a new discussion of the evolutionary history of this group (Schwarz *et al.* in prep).

Acknowledgements. We thank Stéphane Jouve (MNHN) for providing valuable information (including numerous photographs) on yet unpublished material, as well as for fruitful discussions with DS. During the visits of DS to different museums and collections, access and information was provided by Carl Mehling and Ivy Rutzky (both AMNH), Sandra Chapman and Angela Milner (both BMNH), Natalie Bardet (MNHN), Daniel Baudet (MRAC), Daniel Brinkman (YPM) and Walter Joyce (YPM). Thanks for discussions and helpful comments go to Eric Buffetaut (CNRS) and Hans-Peter Schultze (MNB). For their efforts in preparing and curating the specimen of *Dyrosaurus* sp. from the SMNK we thank Olaf Dülfer and René Kastner, as well as Wolfgang Munk for his help with dating the specimen. We are also very grateful for the useful comments and suggestions of an anonymous reviewer and Zulma Gasparini. For this study, DS was funded by the FU Berlin (NaFöG-Programme). Financial support for her stay in the NHM was provided by the European Community with the Access to Research Infrastructure action of the Improving Human Potential Programme (SYS-Resource Program of the NHM), and for her stay in the AMNH and YPM by the Swiss National Science Foundation (SNF).

REFERENCES

ARAMBOURG, C. 1952. Les vertébrés fossiles des gisements de phosphates (Maroc-Algérie-Tunisie). *Service des Mines du Maroc, Rabat, Notes et Mémoires*, **92**, 1–72.

BERGOUNIOUX, F. M. 1956. Les Reptiles fossiles des dépôts phosphatés sud tunisiens. *Annales des Mines et de la Géologie*, **15**, 1–105.

BUFFETAUT, E. 1976. Une nouvelle définition de la famille des Dyrosauridae De Stefano, 1903 (Crocodylia, Mesosuchia)

et ses consequences: inclusion des genres *Hyposaurus* et *Sokotosuchus* dans les Dyrosauridae. *Geobios*, **9**, 333–336.

—— 1978*a*. Crocodilian remains from the Eocene of Pakistan. *Neues Jahrbuch für Geologie und Paläontologie, Abhandlungen*, **156**, 262–283.

—— 1978*b*. Les Dyrosauridae (Crocodylia, Mesosuchia) des phosphates de l'Eocene inférieur de Tunisie: *Dyrosaurus*, *Rhabdognathus*. *Phosphatosaurus*. *Annales de l'Université de Provence, Géologie Mediterranéenne*, **5**, 237–256.

—— 1978*c*. A dyrosaurid (Crocodylia, Mesosuchia) from the Upper Eocene of Burma. *Neues Jahrbuch für Geologie und Paläontologie, Monatshefte*, **1978** (5), 273–281.

—— 1980. Les crocodiliens paleogenes du Tilemsi (Mali): un aperçu systématique. *Palaeovertebrata, Mémoires Jubilaire en Hommage à René Lavocat*, 15–35.

—— and LAUVERJAT, J. 1978. Un Crocodilien d'un type particulier dans le Cénomanien de Nazaré. *Comptes Rendus Sommaire des Seances de la Societe Géologique de France*, **1978** (2), 79–82.

—— BUSSERT, R. and BRINKMANN, W. 1990. A new nonmarine vertebrate fauna in the Upper Cretaceous of northern Sudan. *Berliner Geowissenschaftliche Abhandlungen, A*, **120**, 183–202.

BUSTARD, H. R. and SINGH, L. A. K. 1977. Studies on the Indian gharial *Gavialis gangeticus* (Gmelin) (Reptilia, Crocodylia). Change in terrestrial locomotory pattern with age. *Journal of the Bombay Natural History Society*, **74**, 534–535.

CRUSH, P. J. 1984. A late Upper Triassic sphenosuchid crocodilian from Wales. *Palaeontology*, **27**, 131–157.

DENTON, R. K. Jr, DOBIE, J. L. and PARRIS, D. C. 1997. The marine crocodilian *Hyposaurus* in North America. 375–479. *In* CALLAWAY, J. M. and NICHOLLS, E. L., (eds). *Ancient marine reptiles. Part V. Crocodylia.* Academic Press, San Diego, 501 pp.

DOLLO, L. 1914. Sur la découverte de Téleosauriens tertiares au Congo. *Bulletin de l'Academie Royale des Sciences, des Lettres et des Beaux-arts de Belgique*, **80**, 288–298.

FREY, E. 1988*a*. Anatomie des Körperstammes von *Alligator mississippiensis* Daudin. *Stuttgarter Beiträge zur Naturkunde, Serie A*, **24**, 1–106.

—— 1988*b*. Das Tragsystem der Krokodile – eine biomechanische und phylogenetische Analyse. *Stuttgarter Beiträge zur Naturkunde, Serie A*, **26**, 1–60.

GANS, C. and BOCK, W. J. 1965. The functional significance of muscle architecture – a theoretical analysis. *Ergebnisse der Anatomie und Entwicklungsgeschichte*, **38**, 115–142.

—— and DE VREE, F. 1987. Functional bases of fibre length and angulation in muscles. *Journal of Morphology*, **192**, 63–85.

HOFFSTETTER, R. and GASC, J. P. 1969. Vertebrae and ribs of modern reptiles. 210–310. *In* GANS, C., BELLAIRS, A. D. A. and PARSONS, T. S. (eds). *Biology of the Reptilia, Morphology F, Volume 1*. Academic Press, London, 556 pp.

HUA, S. 1997. Adaptations des crocodiliens mésosuchiens au milieu marin. Thèse de Doctorat de l'Université Paris 6, Paléontologie des Vertébrés. *Mémoires de la Collection des Sciences de la Terre de l'Université Pierre et Marie Curie, Paris*, **97** (16), 211 pp.

—— 2003. Locomotion in marine mesosuchians (Crocodylia): the contribution of the 'locomotion profiles'. *Neues Jahrbuch für Geologie und Paläontologie, Abhandlungen*, **227**, 139–152.

—— and BUFFETAUT, E. 1997. Crocodylia. Introduction. 357–374. *In* CALLAWAY, J. M. and NICHOLLS, E. L. (eds). *Ancient marine reptiles. Part V. Crocodylia*. Academic Press, San Diego, 501 pp.

JOUVE, S. and SCHWARZ, D. 2004. *Congosaurus bequaerti*, a Paleocene dyrosaurid (Crocodyliformes; Mesoeucrocodylia) from Landana (Angola). *Bulletin de l'Institut Royal des Sciences Naturelles de Belgique, Sciences de la Terre*, **74**, 129–146.

KRAUS, R. 1998. The cranium of *Piscogavialis jugaliperforatus* n. gen., n. sp. (Gavialidae, Crocodylia) from the Miocene of Peru. *Paläontologische Zeitschrift*, **72**, 389–406.

LANGSTON, W. Jr 1995. Dyrosaurs (Crocodilia: Mesosuchia) from the Paleocene Umm Himar Formation, Kingdom of Saudi Arabia. *US Geological Survey, Bulletin*, **2093-F**, 1–36.

NORELL, M. A. and STORRS, G. W. 1989. Catalogue and review of the type fossil crocodilians in the Yale Peabody Museum. *Postilla*, **203**, 1–28.

OWEN, R. 1849. Notes on remains of fossil reptiles discovered by Prof. Henry Rogers, of Pennsylvania, U.S., in Green-sand formation of New Jersey. *Quarterly Journal of the Geological Society of London, Proceedings*, **5**, 380–383.

PARRIS, D. C. 1986. Biostratigraphy of the fossil crocodile *Hyposaurus* Owen from New Jersey. *Investigations of the New Jersey State Museum*, **4**, 1–16.

POL, D. 2003. New remains of *Sphagesaurus huenei* (Crocodylomorpha: Mesoeucrocodylia) from the Late Cretaceous of Brazil. *Journal of Vertebrate Paleontology*, **23**, 817–831.

POMEL, A. 1894. Sur le *Dyrosaurus thevestensis*. *Comptes Rendus de l'Academie des Sciences, Paris, D*, **118**, 1396.

SALISBURY, S. W. 2001. A biomechanical transformation model for the evolution of the eusuchian-type bracing system. Unpublished PhD thesis, University of New South Wales, Sydney.

—— and FREY, E. 2001. A biomechanical transformation model for the evolution of semi-spheroidal articulations between adjoining vertebral bodies in crocodilians. 85–134. *In* GRIGG, G. C., SEEBACHER, F. and FRANKLIN, C. E. (eds). *Crocodilian biology and evolution*. Surrey Beatty & Sons, Chipping Norton, 446 pp.

SCHWARZ, D. 2003. Konstruktionsmorphologische und evolutionsbiologische Analyse der Dyrosauridae (Crocodilia). PhD thesis, FB Geowissenschaften, FU Berlin, 426 pp.

STORRS, G. W. 1986. A dyrosaurid crocodile (Crocodylia: Mesosuchia) from the Paleocene of Pakistan. *Postilla*, **197**, 1–16.

SWINTON, W. E. 1930. On fossil reptilia from Sokoto Province. *Geological Survey of Nigeria Bulletins V*, **13**, 9–61.

—— 1950. On *Congosaurus bequaerti* Dollo. *Annales du Musée du Congo Belge, Tervuren, Serie in 8°, Sciences Géologiques*, **4**, 1–60.

TARSITANO, S., FREY, E. and RIESS, J. 1988. On the method of tendon attachment to bone. *Beiträge zum 1. Internationalen Symposium des SFB 230 Natürliche Konstruktionen. Leichtbau in Architektur und Natur vom 26.9. bis 29.9.1988*, **2**, 105–110.

THEVENIN, A. 1911. Le *Dyrosaurus* des phosphates de Tunisie. *Annales de Paléontologie*, **6**, 95–108.

TROXELL, E. L. 1925. *Hyposaurus*, a marine crocodilian. *American Journal of Science*, **9**, 489–514.

VIGNAUD, P. 1995. Les Thalattosuchia, crocodiles marins du Mésozoique: systematique, phylogénétique, paléoécologie, biochronologie et implications paléogéographiques. Thèse de Doctorat de l'Université de Poitiers, Faculté de Sciences Fondamentales et Appliquées, Poitiers, 271 pp.

WESTPHAL, F. 1962. Die Krokodilier des Deutschen und Englischen Oberen Lias. *Palaeontographica A*, **118**, 23–118.